

2
3 Q1 **Targeting the DNA Damage Response Pathways and**
4 Q2 **Replication Stress in Colorectal Cancer**



5 AU Erika Durinikova¹, Nicole M. Reilly^{1,2}, Kristi Buzo^{1,2}, Elisa Mariella^{1,2}, Rosaria Chilà^{2,3}, Annalisa Lorenzato^{1,2},
6 João M. L. Dias^{4,5}, Gaia Grasso^{1,2}, Federica Pisati⁶, Simona Lamba¹, Giorgio Corti^{1,2}, Andrea Degasperis^{4,5},
7 Carlotta Cancelliere¹, Gianluca Mauri^{3,7}, Pietro Andrei^{1,2}, Michael Linnebacher⁸, Silvia Marsoni³,
8 Salvatore Siena^{7,9}, Andrea Sartore-Bianchi^{7,9}, Serena Nik-Zainal^{4,5}, Federica Di Nicolantonio^{1,2},
9 Alberto Bardelli^{1,2}, and Sabrina Arena^{1,2}

10 **ABSTRACT**

11 **Purpose:** Genomic instability is a hallmark of cancer and target-
12 ing DNA damage response (DDR) is emerging as a promising
13 therapeutic strategy in different solid tumors. The effectiveness of
14 targeting DDR in colorectal cancer has not been extensively
15 explored.

16 **Experimental Design:** We challenged 112 cell models recapit-
17 ulating the genomic landscape of metastatic colorectal cancer with
18 ATM, ATR, CHK1, WEE1, DNA-PK inhibitors, in parallel with
19 chemotherapeutic agents. We focused then on ATR inhibitors
20 (ATRi) and, to identify putative biomarkers of response and
21 resistance, we analyzed at multiple levels colorectal cancer models
22 highly sensitive or resistant to this drug.

23 **Results:** We found that around 30% of colorectal cancers,
24 including those carrying *KRAS* and *BRAF* mutations and unre-
25 sponsive to targeted agents, are sensitive to at least one DDR

inhibitor. By investigating on potential biomarkers of response to
ATRi, we found that ATRi-sensitive cells displayed reduced phospho-RPA32 foci at basal level, while ATRi-resistant cells showed increased RAD51 foci formation in response to replication stress. Lack of *ATM* and *RAD51C* expression was associated with ATRi sensitivity. Analysis of mutational signatures and HRDetect score identified a subgroup of ATRi-sensitive models. Organoids derived from patients with metastatic colorectal cancer recapitulated findings obtained in cell lines.

Conclusions: In conclusion, a subset of colorectal cancer refractory to current therapies could benefit from inhibitors of DDR pathways and replication stress. A composite biomarker involving phospho-RPA32 and RAD51 foci, lack of *ATM* and *RAD51C* expression, as well as analysis of mutational signatures could be used to identify colorectal cancer likely to respond to ATRi.

45 **Introduction**

46 DNA damage response (DDR) pathways play a critical role for the
47 growth and survival of cancer cells, and their aberrant regulation is
48 responsible for genomic instability, a well-known cancer hallmark (1).
49 Five major repair pathways including homologous recombination
50 (HR), non-homologous end-joining (NHEJ), base excision repair

(BER), nucleotide excision repair, and DNA mismatch repair (MMR) are modulated by more than 450 different effectors which are involved in the repair of single-nucleotide defects or DNA single-strand and double-strand breaks (ref. 2). Several studies have already elucidated the role of HR defects and their clinical implications in cancers such as those of ovarian, breast, prostate, and pancreatic origin (3). In light of the cross-talk between DNA damage sensing, repair, and cell-cycle checkpoints, a set of DDR inhibitors (DDRi) targeting essential DNA repair pathways was recently developed following the paradigmatic example of PARP inhibition in *BRCAness*-affected cancers (4). Replication stress (RS) represents a cause of DNA damage (5) and elevated levels of RS are often observed in cancer cells, mostly attributed to the presence of oncogenic signaling or to the aberrant regulation of cell-cycle checkpoint activators. Therefore, RS, together with defective DDR, represent a therapeutic opportunity in cancers (6, 7).

Colorectal cancer is the third leading cause for cancer-related death in the Western world and current classification based on loss of a specific DDR function encompasses the distinction into microsatellite stable (MSS) and unstable (MSI) colorectal cancers (8). A subset of colorectal cancer with MSI-high or deficient MMR profiles are effectively treated with immune checkpoint inhibitors (9), while MSS colorectal cancers are mainly subjected to one-size-fits-all chemotherapeutic regimen, often exposing patients to known risk of iatrogenic toxicity in exchange of an unknown chance of clinical benefit. We and others have shown that several targeted agents, including EGFR, HER2, TRK, and BRAF inhibitors, are effective in subsets of patients with MSS colorectal cancer, but response is generally transient owing to the emergence of acquired resistance (10). Moreover, for both patients with MSI and MSS colorectal cancer, available treatments

Q3 ¹Candiolo Cancer Institute, FPO - IRCCS, Candiolo, Torino, Italy. ²Department of Oncology, University of Torino, Candiolo, Italy. ³IFOM, FIRC Institute of Molecular Oncology, Milan, Italy. ⁴Department of Medical Genetics, University of Cambridge, Cambridge, United Kingdom. ⁵Early Cancer Institute, University of Cambridge, Cambridge, United Kingdom. ⁶Histopathology Unit, Cogentech, Milan, Italy. ⁷Department of Oncology and Hemato-Oncology, University of Milan, Milan, Italy. ⁸Clinic of General Surgery, Molecular Oncology and Immunotherapy, University of Rostock, Rostock, Germany. ⁹Niguarda Cancer Center, Grande Ospedale Metropolitano Niguarda, Milan, Italy.

Note: Supplementary data for this article are available at Clinical Cancer Research Online (<http://clincancerres.aacrjournals.org/>).

A. Bardelli and S. Arena contributed as co-senior authors to this article.

Corresponding Authors: Sabrina Arena, Department of Oncology, University of Torino, Strada Provinciale 142, km 3.95, Candiolo, Torino 10060, Italy. Phone: 3901-1993-3223; E-mail: sabrina.arena@unito.it; and Alberto Bardelli, alberto.bardelli@unito.it

Clin Cancer Res 2022;XX:XX-XX

doi: 10.1158/1078-0432.CCR-22-0875

This open access article is distributed under the Creative Commons Attribution-NonCommercial-NoDerivatives 4.0 International (CC BY-NC-ND 4.0) license.

©2022 The Authors; Published by the American Association for Cancer Research

Translational Relevance

The identification of novel effective therapies for patients with colorectal cancer that cannot benefit from targeted or immune treatment represents a pressing need in oncology. Defects in effectors involved in the DNA damage response (DDR) and replication stress response might constitute a potentially targetable vulnerability that has led to the development of new agents (DDR inhibitors, DDRi), currently under phase I–III testing. In this work, we test the sensitivity to seven different types of DDRi in a platform including 112 cell lines representing the molecular landscape of colorectal cancer and in a subset of colorectal cancer organoids. Of note, we identify that up to 30% of colorectal cancer models are sensitive to at least one DDRi and we suggest that the use of a composite biomarker involving phospho-RPA32 and RAD51 foci analysis, lack of ATM and RAD51C expression as well as HRDetect analysis could better stratify colorectal cancer likely to benefit from ATRi.

beyond second-line regimen remain limited owing to the low efficacy and high toxicity burden (11).

Recent works suggest that colorectal cancers carrying defective DNA repair pathways might be amenable to PARP therapeutic targeting (12–14) or drugs targeting RS (15–17), although identification of reliable biomarkers of response and/or stratification approaches still remain a pressing need.

Here, we sought to explore in a more systematic and extended way the efficacy of targeting DDR in colorectal cancer by screening 112 cell lines recapitulating the molecular landscape of colorectal cancer with seven different DDRi. Around 30% of colorectal cancer cell models resulted sensitive to at least one DDRi with addition of observed sensitive pattern to RS inhibitors also in a subset of patient-derived organoids (PDO). In addition, we show how alterations of DDR effectors and the analysis of mutational signatures could be exploited as a “composite” biomarker to identify patients likely to benefit from ATR inhibitors (ATRi), a class of drugs that are currently under advanced clinical development and showing efficacy also as monotherapy (18). Parallel analysis of response to chemotherapeutic agents pinpoints cross-sensitivities with clinically relevant implications.

Materials and Methods

Cell lines and cell authentication

Colorectal cancer cell lines as a part of our biobank were characterized previously (refs. 12, 19, 20; Supplementary Table S1). Each cell line was cultured in its specific media under standard culture conditions and routinely checked for *Mycoplasma* contamination (PCR *Mycoplasma* Detection Kit; ABM). Genetic identity was performed before drug testing and key molecular assays by using the PowerPlex 16 HS System (Promega) through short tandem repeats at 16 different loci (D5S818, D13S317, D7S820, D16S539, D21S11, vWA, TH01, TPOX, CSF1PO, D18S51, D3S1358, D8S1179, FGA, Penta D, Penta E, and amelogenin). Amplicons from multiplex PCRs were separated by capillary electrophoresis (3730 DNA Analyzer; Applied Biosystems) and analyzed using GeneMapperID v.3.7 software (Life Technologies).

DDRIs and chemotherapeutic drugs

5-fluorouracil (5-FU; S1209), oxaliplatin (S1224), SN-38 (S4908), and olaparib (AZD2281, Ku-0059436, S1060) were purchased from

Selleckchem. Berzosertib (ATRi; HY-13902), ceralasertib (ATRi; HY-19323), rabusertib (CHKi; HY-14720), adavosertib (Wee1i; HY-10993), AZD0156 (ATMi; HY-100016), and nedisertib (DNA-PKi; HY-101570) were purchased from MedChemExpress, while MG-132 (474790) was purchased from Merck and hydroxyurea (HU; H8627) from Sigma.

Chemotherapy and DDRi screening

The sensitivity was tested in a 7-day-long proliferation assay. Cells were seeded in 48-well culture plates in different numbers per well depending on a cell line to reach 80%–90% confluency of control wells in the end of the assay. The following day, serial dilutions of oxaliplatin (0.75–12 $\mu\text{mol/L}$), 5-FU (0.625–10 $\mu\text{mol/L}$), SN-38 (1–150 nmol/L), berzosertib (0.65–3 $\mu\text{mol/L}$), ceralasertib (0.215–10 $\mu\text{mol/L}$), rabusertib (0.1–5 $\mu\text{mol/L}$), adavosertib (0.65–3 $\mu\text{mol/L}$), AZD-0156 (0.32–15 $\mu\text{mol/L}$), and nedisertib (0.43–20 $\mu\text{mol/L}$) were added using the Tecan D300e Digital Dispenser. Seven days later, the cell viability was assessed by Cell TiterGlo Luminescent Cell Viability assay (Promega) and measured by the Tecan SPARK M10 plate reader. Viability measured for each treatment condition was normalized to untreated controls. Final data are an average of at least three biological replicates with calculated AUC values. To rank cells’ response within each particular drug, we calculated *Z* score values based on the standard formula.

Genomic DNA extraction, whole-exome sequencing, and bioinformatic analysis

Genomic DNA samples were extracted from each cell line using Maxwell RSC Blood DNA Kit (Promega) and sent to IntegraGen (France) for sequencing. Data analysis was performed in-house following procedures described previously (21).

RNA extraction, sequencing, and bioinformatic analysis

RNA samples were extracted using Maxwell RSC miRNA Tissue Kit (Promega). RNA sequencing (RNA-seq) reads in FASTQ format were aligned to the hg38 version of the human genome using the splice-aware MapSplice aligner. Output BAM files were processed to translate genomic coordinates into transcriptomic ones and remove reads with indels, large inserts, and zero mapping quality before proceeding with transcript and gene quantification using RSEM and GENCODE Release 33 as human gene annotation. In particular, we computed robust fragments per kilobase of transcript per million mapped reads (FPKM) values exploiting the tximport R Bioconductor package (22) and the FPKM function included in the DESeq2 R Bioconductor package (23) starting from RSEM gene-level expected counts and effective lengths obtained for each gene in each sample. The resulting gene expression matrix was subsequently annotated with gene names from the GENCODE annotation file and filtered by applying the following criteria: (i) genes on chrM or chrY pseudoautosomal regions were removed; (ii) genes with FPKM = 0 in >90% analyzed samples or FPKM < 1 in all analyzed samples were considered not expressed and removed; (iii) only protein-coding genes, as defined by the GENCODE annotation file, were selected for subsequent analysis.

Prediction of molecular subtypes

The prediction of CMS and CRIS molecular subtypes was performed after \log_2 transformation of gene expression values using the CMScaller R package and the CRIS classifier R package with default parameters. Cell lines that cannot be confidently assigned to a single subtype (FDR > 5%) were labeled as NA (not available).

181	MSI analysis	240
182	The microsatellite instability (MSI) status was evaluated as	241
183	described previously (12).	242
184	Circos plot generation	243
185	Circular representation of colorectal cancer molecular features was	244
186	generated by combining functions of R packages circlize and	245
187	ComplexHeatmap (24, 25).	246
188	Whole-genome sequencing and mutational signature analysis	247
189	Genomic DNA samples were extracted using ReliaPrep gDNA	248
190	Tissue Miniprep System (Promega) and sent to IntegraGen (France)	249
191	for sequencing. Raw reads were aligned to the human reference	250
192	genome GRCh37/hg19 by bwa-mem (26) and the resulting BAM files	251
193	were used as input for the pipeline developed to assess mutational	252
194	signatures on colorectal cancer cell lines (without matched normal).	253
195	Germline small [single-nucleotide variants (SNV) and Indels] and	254
196	structural variants (SV) were first detected with Strelka (version 2.9.10;	255
197	ref. 27) and Manta (version 1.6.0; ref. 28), executed on tumor-only	256
198	mode, using default parameters. Variants with “PASS” filter flag were	257
199	taken into the next step. Common SNVs and Indels located within a	258
200	genomic window of common Indels that started 4 bp upstream and	259
201	ended 4 bp downstream were removed along with recurrent variants in	260
202	the cohort. SVs were discarded if fully located within the same genomic	261
203	region of common SVs from the same class (tandem duplications,	262
204	deletions, inversions, and translocations). So-called common variants	263
205	were compiled from four databases available in the literature (29–32).	264
206	Copy-number alterations (CNA) were called with ASCAT (33)	265
207	using read counts at genomic positions present in 1000 Genome SNPs	266
208	(phase III, release 83; ref. 34). Read counts from tumor samples were	267
209	normalized using read count medians of all colorectal cancer cell lines	268
210	at each genomic position.	269
211	Mutational signature analysis was performed using SignatureTools	270
212	software package (35) on the filtered variants. SignatureExtraction (35)	271
213	algorithm was adapted to additionally extract base substitution signa-	272
214	tures that have not been classified as known signatures but are	273
215	present in these unmatched colorectal cancer cell lines. Variants <i>r</i> in	274
216	these “novel” signatures are likely to represent outstanding germline	275
217	variants or artifacts introduced in the various steps of cell line culturing	276
218	and sequencing that were not discarded in previous steps. Cosmic base	277
219	substitution signatures (v3.2; ref. 36) 1, 2, 3, 5, 6, 7a, 7b, 8, 10a, 10b, 11,	278
220	13, 14, 15, 17a, 17b, 18, 20, 26, 28, 30, 36, 37, 40, 44, known to be	279
221	associated with DDR pathways or observed in colorectal cancer, were	280
222	considered on signature extraction with SignatureFit. The two “novel”	281
223	signatures were also added to the list to allow an independent	282
224	extraction of signature associated with outstanding germline variants	283
225	and artifacts.	284
226	The HRDetect model suitable for mutational signature analysis	285
227	carried out with samples without matched normal using tumor	286
228	variants and CNAs calls filtered with the pipeline described above	287
229	was derived on the same training and validation dataset of the original	288
230	model (37). In this case, only one “novel” signature was added to	289
231	represent outstanding germline variants. The resulting HRDetect	290
232	model predicted BRCA1/BRCA2 deficiency with a sensitivity and	291
233	specificity of approximately 91% in 560 breast cancers for a proba-	292
234	bilistic cutoff of 0.5. The same model was used to estimate HRDetect	293
235	score in the colorectal cancer cell lines.	294
236	CRISPR-mediated ATM knockout	295
237	To knockout (KO) <i>ATM</i> in SW480 cell line, we used the genome	296
238	editing one vector system (lentiCRISPR-v2; Addgene #52961).	297
	Single-guide RNAs (sgRNA) were designed using the CRISPR tool	240
	(http://crispr.mit.edu) and the following sgRNA sequences were	241
	used: sgRNA1: CCAAGGCTATTCAGTGTGCG; sgRNA2: TGA-	242
	TAGAGCTACAGAACGAA. Annealed sgRNA oligonucleotides	243
	targeting mouse <i>ATM</i> were cloned into Bsmbl lentiCRISPR-v2	244
	plasmid, as described previously (38). SW480 cells were transfected	245
	with lentiCRISPR-v2 vector plasmid (using the same guides as	246
	described above). Transfection was carried out using Lipofectamine	247
	3000 (Life technologies) and Opti-MEM (Invitrogen), according to	248
	the manufacturer’s instructions. After 48 hours, cells were incu-	249
	bated with puromycin (Sigma-Aldrich) for 4 days and subsequently	250
	single-cell diluted in 96-well plates. We selected clones that lacked	251
	<i>ATM</i> and confirmed the absence of the protein and Cas9 based on	252
	Western blot analysis. Testing of <i>ATM</i> KO clones with berzosertib	253
	and ceralasertib was performed in 96-well plates, where cells were	254
	treated for 6 days at the indicated concentrations and cell viability	255
	was assessed by Cell TiterGlo Luminescent Cell Viability assay	256
	(Promega). Treated wells were normalized to untreated wells. Final	257
	results are expressed as an average of three biological replicates.	258
	Immunofluorescence	259
	Cells seeded at a density of $1-2 \times 10^5$ cells on a glass coverslip in a	260
	24-well plate were treated the next day with HU at a concentration of	261
	2.5 mmol/L for indicated times. At the end of treatment, cells were	262
	fixed in 4% paraformaldehyde for 20 minutes at room temperature and	263
	permeabilized with 0.1% Triton-X100 in PBS for 5 minutes. Cells were	264
	incubated at room temperature with 1% BSA in PBS for 30 to 60	265
	minutes, followed by incubation overnight at 4°C with the following	266
	primary antibodies diluted in PBS containing 1% of BSA: anti-phos-	267
	pho-RPA32 (Ser33; Bethyl Laboratories A300-246A; 1:500); anti-	268
	phospho-CHK1 (Ser345; Cell Signaling Technology 2348S; 1:400);	269
	anti-phospho-Histone H2AX (Ser139; Bethyl Laboratories A300-	270
	081A; 1:600); anti-RAD51 (Millipore ABE257; 1:100). After washing,	271
	cells were fluorescently labeled with an Alexa Fluor 555 or Alexa Fluor	272
	488 donkey anti-rabbit antibody (Molecular Probes; 1:400) for 1 to	273
	2 hours at room temperature. Nuclei were stained with DAPI. A Leica	274
	DMI6000B fluorescence microscope (Leica Microsystems) under a	275
	40× dry objective was used to detect pRPA32, pCHK1, γ H2AX, and	276
	RAD51 foci or pan-nuclear staining. For detection of nuclear-localized	277
	foci, images were captured at 10 individual z-planes and were merged	278
	using the “Z Project” function in ImageJ. Individual nuclei were scored	279
	for foci positivity as identified based upon signal intensity above	280
	general background staining levels and present within the nucleus as	281
	assessed by DAPI staining. Cells containing ≥ 5 distinct foci were	282
	defined as foci positive, and the percentage of positive nuclei was	283
	calculated as [(number of foci-positive nuclei)/(number of nuclei	284
	scored)]*100. For pan-nuclear staining, images were captured at the	285
	focal plane. Individual nuclei were scored for positivity using the	286
	ImageJ “analyze particles” function and the percentage of positive	287
	nuclei was calculated as [(number of foci-positive nuclei)/(number of	288
	nuclei scored)]*100. A minimum of 400 nuclei per sample were scored.	289
	Olaparib screening	290
	The response to olaparib in a long-term proliferation assay (10–	291
	14 days) was retrieved from our previous publication (12). For all the	292
	cell lines which were not tested previously, we provided the very same	293
	experimental setup.	294
	Organoid culture and drug screening	295
	Tumor samples were obtained from patients treated at Niguarda	296
	Cancer Center (Milan, Italy) after written consent and the study was	297

300 conducted in accordance with the local Independent Ethical Com- 358
 301 mittee (protocol 194/2010). The PDOs and patient-derived xeno- 359
 302 Q8 organoids were established and maintained in the culture as described in 360
 303 full details in ref. 12. 361

304 Organoids were enzymatically dissociated using TrypLE Express 362
 305 Enzyme for 10 to 20 minutes at 37°C to obtain single-cell suspensions 363
 306 and seeded at a density of 4,000 to 6,000 cells per well in 96-well plates 364
 307 precoated with basement membrane extract (BME; Cultrex BME Type 2; 365
 308 Amsbio) overlaid with 100 µL of 2% BME/growth media. The 366
 309 Q9 treatment with drugs started on day 4 after seeding when formed 367
 310 growing organoids were visible. Organoids were treated in fresh 150 µL 368
 311 medium containing 2% BME with increasing doses of six different 369
 312 DDRi or SN-38 in technical quadruplicates, covering physiologic 370
 313 concentrations of the drugs. Treatment was done automatically by 371
 314 Tecan D300e Digital Dispenser. A total of 4 µmol/L MG-132 was used 372
 315 as a positive control, DMSO served as negative control. The viability 373
 316 was assayed at the end of the experiment after 7 days of treatment by 374
 317 CellTiter-Glo Luminescent Cell Viability assay (Promega) with mod- 375
 318 ifications. Briefly, plates were equilibrated at room temperature for 30 376
 319 minutes and reagent was mixed 1:1 with organoid media. Organoids 377
 320 were then subjected to the lysis by vigorous shaking for 25 minutes, and 378
 321 readout was done by plate reader Tecan SPARK 10M. The raw CTG 379
 322 values were normalized to the mean of the DMSO control wells on a 380
 323 per-plate basis. The control wells (positive and negative) were used to 381
 324 calculate Z factors to indicate the quality of the data generated in the 382
 325 screening plate (as a standard rule, data obtaining Z factor >0.4 are 383
 326 acceptable). All experiments were independently repeated at least two 384
 327 times, and final results are expressed as an average of biological 385
 328 replicates. 386

329 The formula used to calculate Z factor:

$$330 \quad Z \text{ factor} = 1 - \frac{3 * \text{standard deviation(negative control)} + 3 * \text{standard deviation(positive control)}}{\text{average(negative control)} - \text{average(positive control)}}$$

332

333 **Immunofluorescence in organoids**

334 Q10 Untreated and HU-treated (at a concentration of 2.5 mmol/L for 387
 335 24 hours) organoids, grown on chamber slides (Falcon Culture- 388
 336 Slides) previously precoated with BME (Cultrex BME Type 2; 389
 337 Amsbio), were fixed in 4% paraformaldehyde in PBS solution for 390
 338 30 minutes at room temperature and permeabilized with 0.5% 391
 339 Triton-X100 in PBS for 30 minutes at room temperature. Organoids 392
 340 were then incubated with 1% BSA in PBS for 60 minutes, followed 393
 341 by incubation overnight with the following primary antibodies 394
 342 diluted in PBS containing 1% of BSA and 1% of donkey serum: 395
 343 anti-RAD51 (Millipore ABE257; 1:100), anti-phospho-RPA32 396
 344 (Ser33; Bethyl Laboratories A300-246A; 1:500), and anti-phos- 397
 345 pho-Histone H2AX (Ser139; Bethyl Laboratories A300-081A; 398
 346 1:600). After washing, organoids were fluorescently labeled with 399
 347 Alexa Fluor 488 donkey anti-rabbit antibody (Invitrogen) diluted 400
 348 1:400 in PBS containing 1% BSA and 1% donkey serum for 1 to 401
 349 2 hours. Nuclei were stained with DAPI. Slides were then mounted 402
 350 using the fluorescence mounting medium (Dako) and analyzed 403
 351 using a confocal laser scanning microscope (TCS SPE II, Leica). 404

352 **IHC in cell lines and organoids**

353 For IHC analyses, biological samples were sliced in 4-µm-thick 405
 354 sections, deparaffinized in xylene, and rehydrated through decreasing 406
 355 concentrations (100%, 95%, 80%, and 70%) of ethyl alcohol, then 407
 356 rinsed in distilled water. Antigen retrieval was carried out using 408

358 preheated target retrieval solution for 30 minutes. Endogenous per- 359
 360 oxidase activity was quenched with 0.3% hydrogen peroxide in distilled 360
 361 water. Slides were treated with 1% BSA and 2% FBS in PBS 361
 362 and then incubated in a closed humid chamber overnight at 4°C with 362
 363 anti-RAD51C (1:1,000, Thermo Fisher Scientific, PA5-75307) or anti- 363
 364 ATM antibody (1:100 in case of cell lines; 1:500 in case of PDOs, 364
 365 Abcam ab32420). The antibody binding was detected using a polymer 365
 366 detection kit (GAR-HRP, Microtech) followed by a diaminobenzidine 366
 367 chromogen reaction (Peroxidase substrate kit, DAB, SK-4100; Vector 367
 368 Lab). All sections were counterstained with Mayer's Hematoxylin 368
 369 (Diapath, C0305) and visualized using a bright-field microscope (Leica 369
 DM750).

370 **Western blotting**

371 Cells were seeded in 6-well culture plates (seeding number was 371
 372 adjusted for each cell line to reach optimal confluency by the end of the 372
 373 experiment), treated next day with 1 µmol/L ATRi ceralasertib for 373
 374 24 hours, 2.5 mmol/L HU for 4 hours, and their combination for 374
 375 24 hours (HU was added for the last 4 hours of the treatment). Cells 375
 376 were subsequently lysed in using boiling SDS buffer [50 mmol/L Tris- 376
 377 HCl (pH 7.5), 150 mmol/L NaCl, and 1% SDS] to extract total cellular 377
 378 proteins, quantified by the BCA Protein Assay Reagent kit (Thermo 378
 379 Fisher Scientific), and prepared using LDS and Reducing Agent 379
 380 (Invitrogen). Western blot analysis was performed with Enhanced 380
 381 Chemiluminescence System (GE Healthcare) and peroxidase- 381
 382 conjugated secondary antibodies (Amersham). The following primary 382
 383 antibodies were used for Western blotting: anti-phospho-RPA32 383
 384 (Ser33; Bethyl Laboratories A300-246A; 1:1,000), anti-RPA32 (Abcam 384
 385 AB252861; 1:2,000), anti-RPA32 (S4/S8; Bethyl Laboratories A300- 385
 386 245A; 1:3,000), anti-ATR (Cell Signaling Technology, 13934S; 386

387 1:1,000), anti-phospho-CHK1 (Ser345; Cell Signaling Technology, 387
 2348S; 1:1,000), anti-CHK1 (Cell Signaling Technology, 2360S; 388
 1:1,000), anti-phospho-Histone H2AX (Ser139; Cell Signaling Techn- 389
 ology, 80312S; 1:1,000), anti-H2AX (Cell Signaling Technology, 390
 7631S; 1:1,000), anti-phospho-DNA-PK (Ser2056; Cell Signaling 391
 Technology, 68716S; 1:1,000), anti-DNA-PK (Cell Signaling Technol- 392
 ogy, 12311S; 1:1,000), anti-RAD51 (Genetex GTX70230; 1:1,000), and 393
 anti-HSP90 (Santa Cruz Biotechnology, SC-7947; 1:1,000). In the 394
 Western blot screening analysis, we used following antibodies: anti- 395
 ATM (Cell Signaling Technology, 2873S; 1:1,000); anti-P53 (Sigma- 396
 Aldrich p5813; 1:1,000); anti-RAD51C (Santa Cruz Biotechnology SC- 397
 56214; 1:1,000) and anti-Vinculin (MERCK 05-386; 1:3,000). Detec- 398
 tion of the chemiluminescent signal was performed with ChemiDoc 399
 Imaging System (Bio-Rad). 400

401 **In vivo xenograft models**

402 Animal procedures were approved by the Ethical Commission of 402
 403 the Institute FIRC of Molecular Oncology (IFOM, Milan, Italy) and by 403
 404 the Italian Ministry of Health, and were performed in accordance with 404
 405 institutional guidelines and international law and policies. Mice were 405
 406 obtained from Charles River and were maintained under pathogen- 406
 407 free conditions in individually ventilated cages and with free access to 407
 408 food and water. During the experiment, investigators were not blinded. 408
 409 Mice were checked daily for signs of illness and distress. 409

410 Four-to five weeks old female NOD-SCID mice were used. Tumor 410
 411 size was measured twice a week and calculated using the formula $V =$ 411

414 $(d^2 \times D)/2$ (d = minor tumor axis; D = major tumor axis) and reported
415 as tumor volume (mm^3 ; mean \pm SEM of individual tumor volumes).

416 Exponentially growing C80 cells were resuspended in a mixture of
417 50% PBS and 50% Matrigel (Corning) and injected subcutaneously in
418 the flank (5×10^6 cells per mouse). Once the tumors reached a volume of
419 approximately $100/200 \text{ mm}^3$, mice were randomized (at least 8 per
420 group) to receive ceralasertib (prepared in 10% DMSO, 40% PEG300,
421 5% Tween80, and 45% sterile water) or vehicle. The drug solution and
422 the vehicle control were administered by oral gavage daily at 50 mg/kg
423 for 3 weeks.

424 Statistical analysis

425 Results were expressed as means \pm SEM or SD. Statistical
426 significance was evaluated by unpaired t test or Mann-Whitney
427 test as indicated using GraphPad Prism software. $P < 0.05$
428 was considered statistically significant (*, $P < 0.05$; **, $P < 0.01$;
429 ***, $P < 0.001$; ****, $P < 0.0001$).

430 Data availability statement

431 The datasets generated during and/or analyzed during the current
432 study are available from the corresponding author on reasonable
433 request.

434 Results

435 Selection of cell line models recapitulating the genomic 436 landscape of colorectal cancer

437 We previously tested a panel of 99 MSS colorectal cancer cell lines
438 enriched for *KRAS* and *BRAF* alterations and identified a subset
439 of tumors (around 13%) displaying sensitivity to the PARP inhibitor
440 (PARPi) olaparib (12). In this work, we have studied a dataset of
441 112 cell lines, which include not only the majority of those previously
442 tested with olaparib, but also an additional set of *EGFR/RAS/BRAF/*
443 *PIK3CA* wild-type and MSI cell lines which were selected to parallel
444 the molecular and transcriptional landscape of colorectal cancer
445 (refs. 39, 40; Fig. 1A; Supplementary Table S1). Overall, this panel
446 includes 31 cell lines recently derived from tumor biopsy or surgical
447 colorectal cancer samples, as well as from patient-derived xenografts,
448 for which the clinical annotation is available (refs. 20, 41; Fig. 1A;
449 Supplementary Table S1).

450 Systematic targeting of DDR pathways in colorectal cancer 451 preclinical models

452 To establish the fraction of colorectal tumors sensitive to DDR
453 pathway inhibitors, we screened colorectal cancer cell lines with drugs
454 targeting key DDR proteins, namely ATM, ATR (two distinct inhibi-
455 tors), CHK1, WEE1, and DNA-PK (Fig. 1B and Fig. 2; Supplemen-
456 tary Fig. S1; ref. 7). For ATR blockade, we employed berzosertib and
457 ceralasertib, because both inhibitors are undergoing clinical develop-
458 ment for several solid tumors with varying dosing protocols and
459 administration routes (refs. 17, 42; Fig. 1B and Fig. 2; Supplementary
460 Fig. S1).

461 We also assessed sensitivity to the PARPi olaparib in cell models that
462 were not included in our previous study (ref. 12; Fig. 2). In addition, we
463 tested sensitivity of the colorectal cancer cell platform with the three
464 most used standard-of-care cytotoxic drugs in colorectal cancer,
465 namely, 5-FU, SN-38 (the active metabolite of irinotecan), and oxa-
466 liplatin, leading to the identification of additional responsive colorectal
467 cancer lines (Fig. 2).

468 Cell-specific and variable levels of response to chemotherapy were
469 noted (Fig. 2); an overlapping pattern of response was observed

471 between SN-38 and the ATRi ceralasertib and berzosertib (Spearman
472 correlation $r = 0.52$ and 0.43 , respectively; $P < 0.0001$; Fig. 2; Sup-
473plementary Fig. S2A and S2B).

474 RS is a targetable vulnerability in colorectal cancer

475 Drug screening revealed that around 30% of colorectal cancer lines
476 were sensitive to DDRi, with 25% cases being particularly susceptible
477 to ATR inhibition. These values are based on viability $<35\%$ at the
478 clinically relevant concentration of $1 \mu\text{mol/L}$ of the ATRi ceralasertib
479 (Fig. 2). Cross-sensitivity to the two ATRi berzosertib and ceralasertib
480 was evident (Spearman correlation $r = 0.78$; $P < 0.0001$), thus
481 validating the screening (Supplementary Fig. S2C). Pathway sensitivity
482 was also maintained with CHK1 and WEE1 inhibition through
483 rabusertib and adavosertib treatment, respectively, thus revealing a
484 broad dependency to the RS pathway in a subset of colorectal cancer
485 models (Fig. 2; Supplementary Fig. S3A–S3D).

486 We considered that ATRi are in advanced clinical development and
487 appear to show effectiveness as monotherapy (18), while ATMi and
488 DNA-PKi appear to be more effective when combined with targeted,
489 radio- or chemo-based therapies (43, 44). Accordingly, we focused on
490 understanding the impact of RS on response to the ATR blockade in
491 colorectal cancer.

492 We used HU to trigger RS in colorectal cancer cells and we
493 initially assessed pathway activation by immunofluorescence anal-
494 ysis on four ATRi-sensitive and four ATRi-resistant cell lines
495 (Supplementary Fig. S4). We evaluated the role of different DDR
496 effectors on RS, such as γH2AX , a marker of DNA damage (45),
497 activation of replication Protein A (phospho-RPA32), a heterotri-
498 meric protein which recruits DDR effectors to the damage site to
499 initiate the RS response (46), and the phosphorylated form of CHK1
500 (pCHK1 S345), a direct ATR target involved in cell-cycle modu-
501 lation (ref. 47; Supplementary Fig. S4).

502 Induction of RS by HU-triggered DNA damage in both ATRi-
503 sensitive and ATRi-resistant cells, as shown by increased levels of
504 γH2AX and pCHK1 (Supplementary Fig. S4A and S4B). Levels of
505 phosphoS33-RPA32, a residue directly phosphorylated by ATR (48),
506 increased upon HU treatment in both groups (Supplementary
507 Fig. S4C, pan-nuclear signal). We assessed basal levels of pRPA32
508 foci as an indicator of endogenous RS and we found that ATRi-
509 resistant cells showed significantly higher basal pRPA32 foci with
510 respect to the sensitive lines (Supplementary Fig. S4D). Next, we
511 measured RAD51 foci formation upon HU treatment and found that
512 it was significantly increased in ATRi-resistant cells after HU com-
513 pared with ATRi-sensitive cells (Supplementary Fig. S4E). Intrigued by
514 these findings, we extended the analysis to 16 additional models and
515 performed two independent biological experiments. This analysis
516 confirmed that ATRi-resistant colorectal cancer cells display higher
517 basal levels of pRPA32 foci (Fig. 3A–C) and increased levels of RAD51
518 foci formation upon HU treatment (Fig. 3D–F; Supplementary
519 Fig. S5) respect to ATRi-sensitive cells.

520 To further evaluate the impact of RS on the DDR signaling path-
521 ways, we performed biochemical analysis in cells treated with the ATRi
522 ceralasertib, HU, or their combination (Fig. 4). Considering pCHK1 as
523 a marker of ATR pathway activation, we found that this protein was
524 equally activated in ATRi-sensitive and ATRi-resistant lines upon HU
525 treatment, thus mirroring what was previously observed by immu-
526 nofluorescence assay. However, DNA damage, as assessed by γH2AX
527 accumulation, was already evident upon ATRi treatment only in
528 sensitive cells. In addition, upon 24 hours treatment with ATRi,
529 sensitive cells revealed co-activation of phospho-DNA-PK, further
530 confirmed by measuring RPA32 phosphorylation on S4/S8

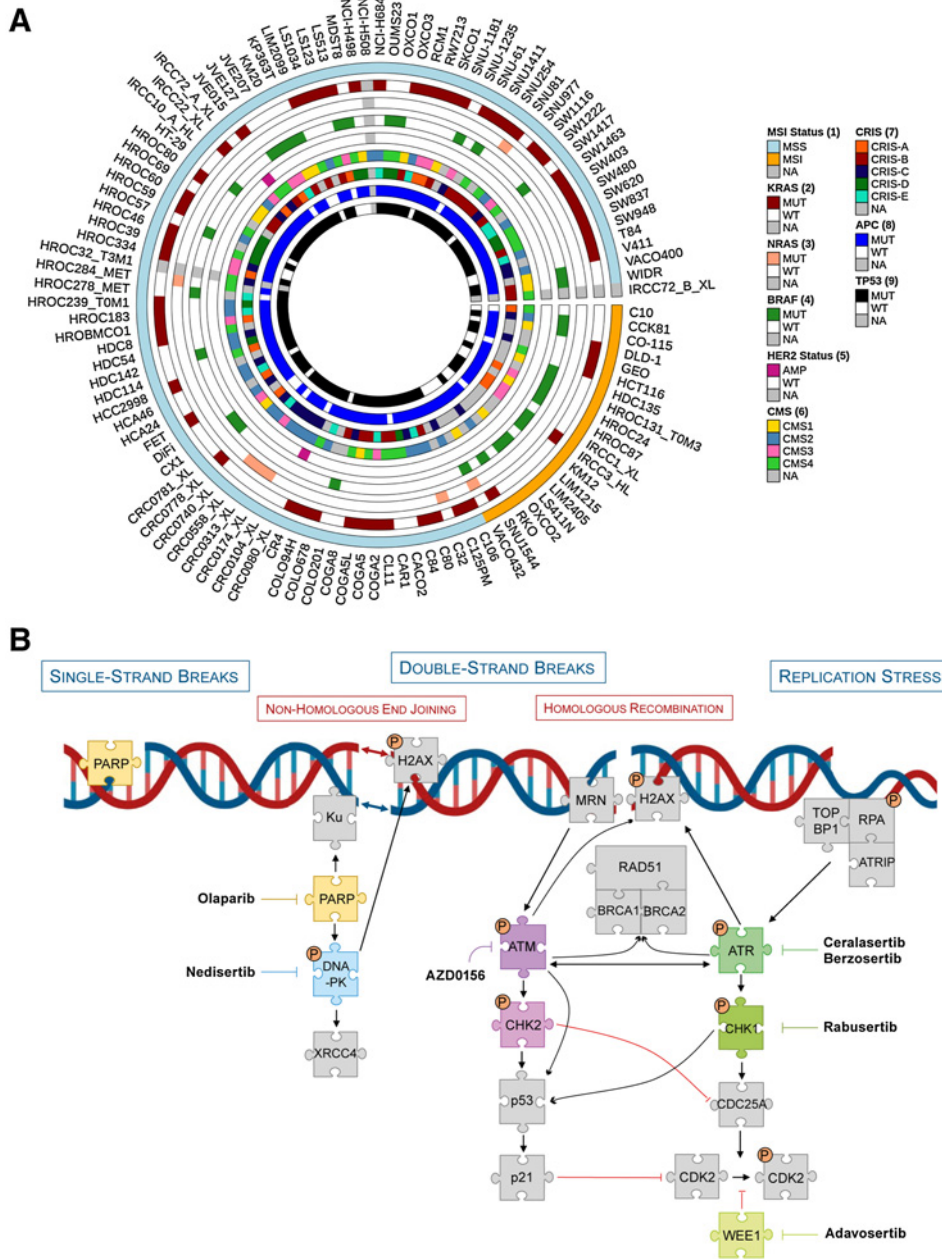


Figure 1. Selection of cell line models representing the genomic landscape of colorectal cancer and scheme of the DDR pathways with their actionable targets. **A**, Circos plot representing the mutational status of a selected panel of 112 colorectal cancer cell lines enriched for *RAS* and *BRAF* mutations or other alterations conferring resistance to anti-EGFR blockade. The *HER2*, *APC*, and *TP53* genetic status is also reported. MUT, mutant; WT, wild type. The distribution of microsatellite status and representation of transcriptional (CRIS) and molecular (CMS) subtypes in cell lines is also shown. MSS, microsatellite stable; MSI, microsatellite instability. NA, not available. **B**, Schematic representation with key players of DDR is shown along with the DDRs currently undergoing clinical development.

Q13

533 residues (49). While S4/S8 residues were already activated upon
 534 treatment with single-agent ATRi or HU in ATRi-sensitive cells, these
 535 residues were phosphorylated in ATRi-resistant cells only when HU-
 536 based treatment was administered. A similar pathway of activation was
 537 also observed for pRPA32-S33 residue (Fig. 4), highlighting a clear
 538 ATR dependency in ATRi-sensitive cells to cope with RS.

Identification of biomarkers of response to ATR pathway inhibitors in colorectal cancer

539 Predictive biomarkers are needed to stratify patients likely to
 540 respond to ATR pathway inhibitors, but research efforts in malignan-
 541 cies other than colorectal cancer have achieved modest results (17, 42).
 542 To fill this gap, we initially performed bioinformatic analysis on
 543 genomic, RNA-seq, and proteomic data gathered from the colorectal
 544
 545

cancer CRC cell lines coupled with pharmacogenomic response to
 ATM, ATR, CHK1, WEE1, and DNA-PK inhibitors. In addition to
cMYC, *RAS*, and *cyclin E* (*CCNE1* and *CCNE2*; Supplementary Figs.
 S6–S8), whose aberrant activation is known to trigger RS in other
 tissues (50), we included other genes involved in carcinogenesis and in
 cell-cycle control (Supplementary Figs. S9 and S10). In general, in our
 cohort, we could not find any robust and statistically significant
 correlations between response to ATR pathway inhibitors (ATRi,
 CHKi, WEEi) and genomic alterations in the subset of DDR/cell-
 cycle genes analyzed in colorectal cancer models.

We then evaluated *TP53*, a tumor suppressor gene involved in the
 cell-cycle control and DDR activation (51). No correlation was found
 between response to ATRi and genetic alterations of *TP53* defined as
 functionally relevant according to the p53.iarc.fr database (see

547
 548
 549
 550
 551
 552
 553
 554
 555
 Q15,556
 557
 558
 559
 560

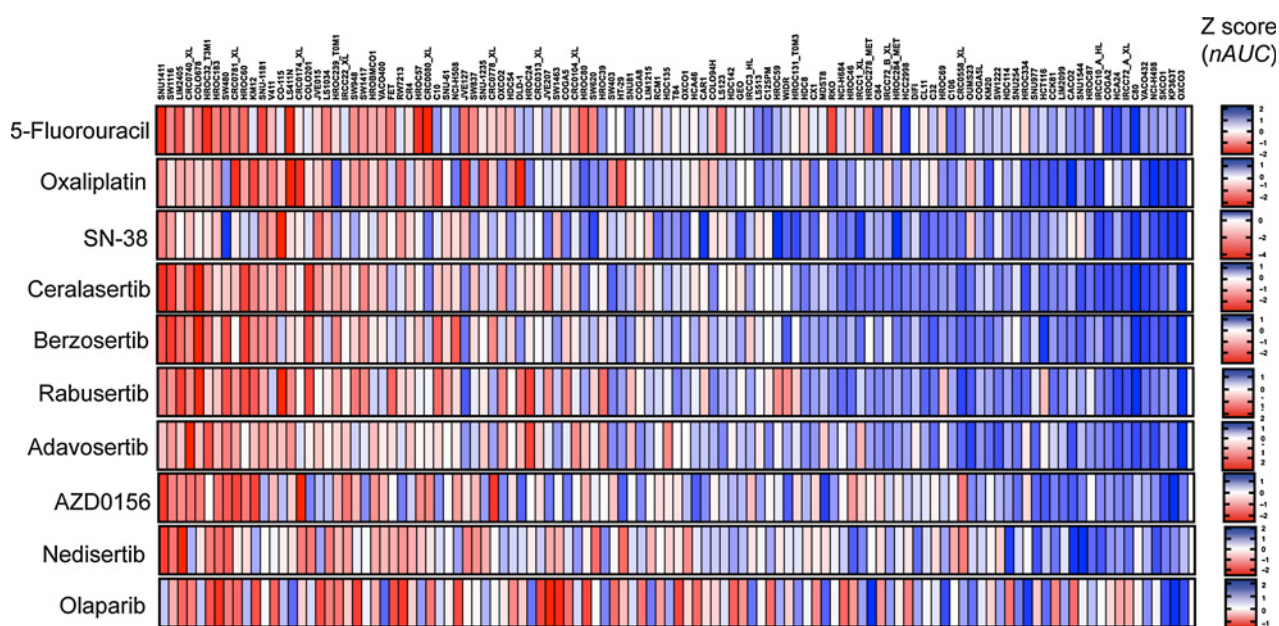


Figure 2. Response profiles to DDRis and chemotherapeutic agents in colorectal cancer cell models. Heatmap representing pharmacoresponse of 112 colorectal cancer cell lines to three chemotherapeutic drugs and seven different DDRis (two of which target ATR). Cells were treated with monotherapy and cell proliferation was assessed after 7 days of treatment. All experiments were repeated in at least three biological replicates with technical triplicates, and final data are expressed as their average. Viability results were expressed as Z scores calculated from normalized AUC (nAUC) values for each individual drug. The red shades represent cells' resistance while the blue scale shows sensitivity to the specific drug. Values for olaparib response have been partly retrieved from our previous publication (12).

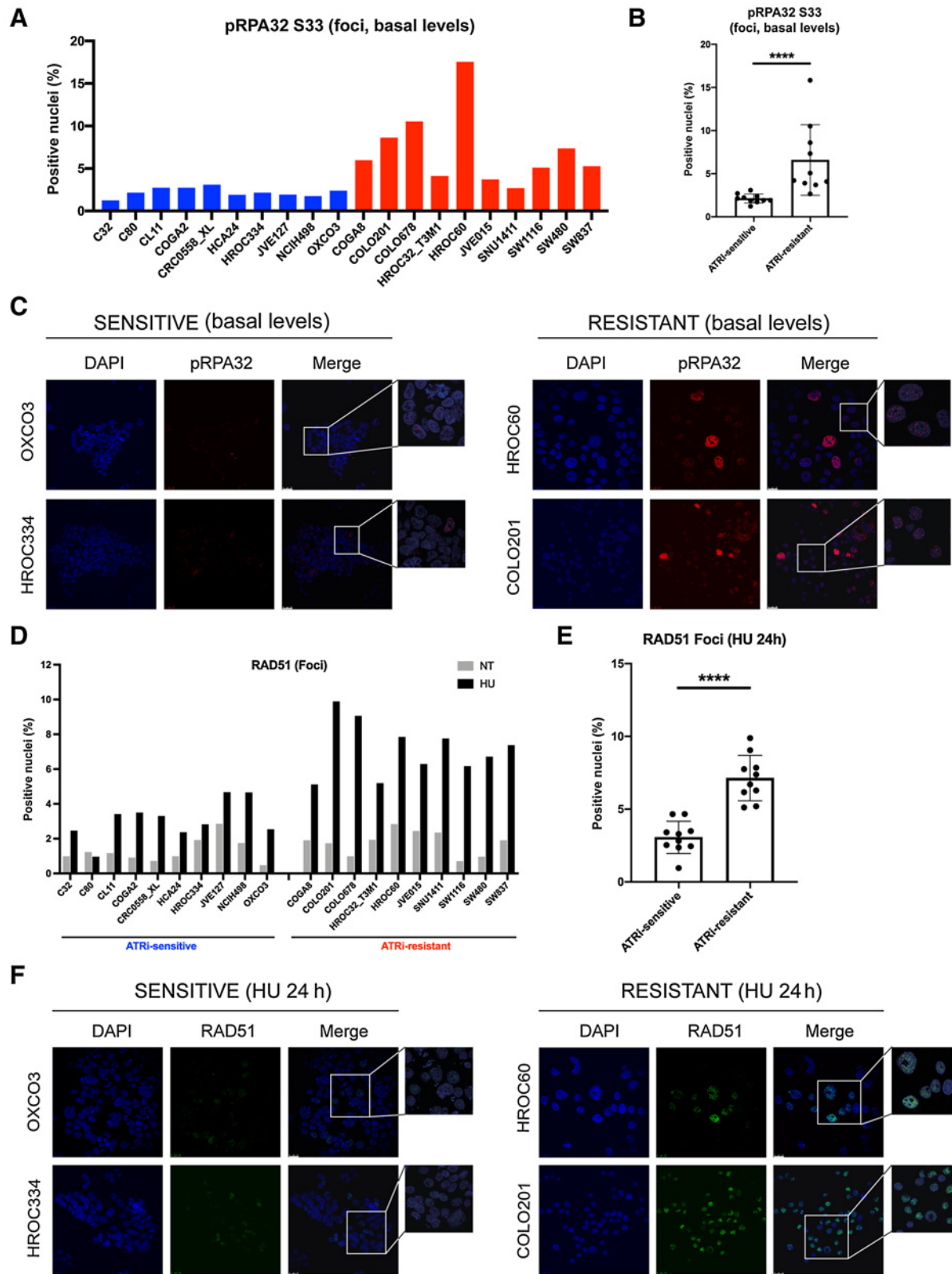
563 Materials and Methods) or p53 protein loss (Supplementary Figs. S9,
 564 S10, S11A, and S11B).
 565 We next analyzed alterations of the *ATM* gene and loss of ATM
 566 protein, which are known to confer sensitivity to ATRi in other tumor
 567 types such as prostate and pancreatic cancer (52, 53).
 568 Distribution of SNVs in the *ATM* sequence was not associated with
 569 ATRi sensitivity (Supplementary Fig. S9A and S9B), while colorectal
 570 cancer cells showing ATM protein loss (tested both by Western blot
 571 and IHC analysis) were clearly sensitive to ATRi (Fig. 5A; Supple-
 572 mentary Fig. S12A and S12B). This observation was confirmed
 573 when we extended the analysis to an additional dataset of 129
 574 colorectal cancer cell lines that are part of our colorectal cancer cell
 575 bank collection (Supplementary Fig. S12C), again we found that
 576 ATM protein loss is invariably associated with sensitivity to ATRi
 577 (Supplementary Fig. S12D).
 578 To mechanistically confirm these findings, we used CRISPR-
 579 mediated gene editing to generate *ATM* KO in SW480 colorectal
 580 cancer cells, which are resistant at the clinically relevant ATRi (cer-
 581 alasertib) concentration of 1 μmol/L (Fig. 5B and C). We isolated two
 582 independent clones from two different guides (guide 1 and 2, clones
 583 1.4, 1.7, 2.2 and 2.3) and all of them showed sensitivity to ATR
 584 inhibition compared with isogenic parental controls, confirming
 585 previous work showing that *ATM* is a fundamental player driving
 586 DDR and RS response (ref. 54; Fig. 5D).
 587 We then considered whether different cell lines that are highly
 588 sensitive to PARP inhibition as shown in our previous work (12) were
 589 also sensitive to ATR inhibition, suggesting that HR deficiency might
 590 also represent a mechanism of sensitivity to RS (Supplementary
 591 Fig. S13A). KP363T, HROC334, and HROC278MET exhibited the
 592 highest sensitivity to olaparib (12) and were also sensitive to ATRi.
 593 Although we were not able to identify potentially pathogenic SNVs in

595 DDR genes in these cells, when we considered RNA-seq and protein
 596 analysis we found out that all of them had no or very low levels of
 597 RAD51C expression (Supplementary Fig. S13B and S13C), a RAD51
 598 paralog whose loss is a well-known mechanism of PARPi sensitivity in
 599 breast and gastric cancer (55). The HROC87 cells which express very
 600 low RAD51 levels (Supplementary Fig. S13D) were also sensitive to
 601 ATRi (Supplementary Fig. S13A).

Analysis of mutational signatures and response to DDRis in colorectal cancer cell lines 602 603

604 Mutational signatures are the imprints of DNA damage and repair
 605 processes that are in place over the course of tumorigenesis (56).
 606 Several mutational signatures have been shown to be the direct
 607 outcome of DNA repair deficiencies and have been proposed as
 608 biomarkers of targetable pathway abnormalities (57). To understand
 609 whether mutational signatures highlighted sensitivity to ATRi inhi-
 610 bition, we undertook whole-genome sequencing of 28 lines, choosing
 611 among the most ATRi-sensitive and ATRi-resistant cells. Next, we
 612 obtained all single-base substitution mutations relative to the refer-
 613 ence human genome and performed mutational signature analysis as
 614 reported previously (35) and explored relationships with the cer-
 615 alasertib blockade.

616 Mutational signature analysis (Supplementary Table S2) revealed
 617 four cases with MSI (CO-115, KM12, SNU1544, and VACO432) and
 618 one case (HCA24) with alteration in polymerase proofreading.
 619 These are well-described DNA repair abnormalities with known
 620 potential sensitivities to immune checkpoint therapies and have
 621 distinct hypermutator phenotypes. These five samples have the highest
 622 tumor mutational burdens within the cohort. Excluding these five
 623 cases, we explored mutational signatures of the rest of the cohort and
 624 found that cell lines with increased sensitivity to ceralasertib have a



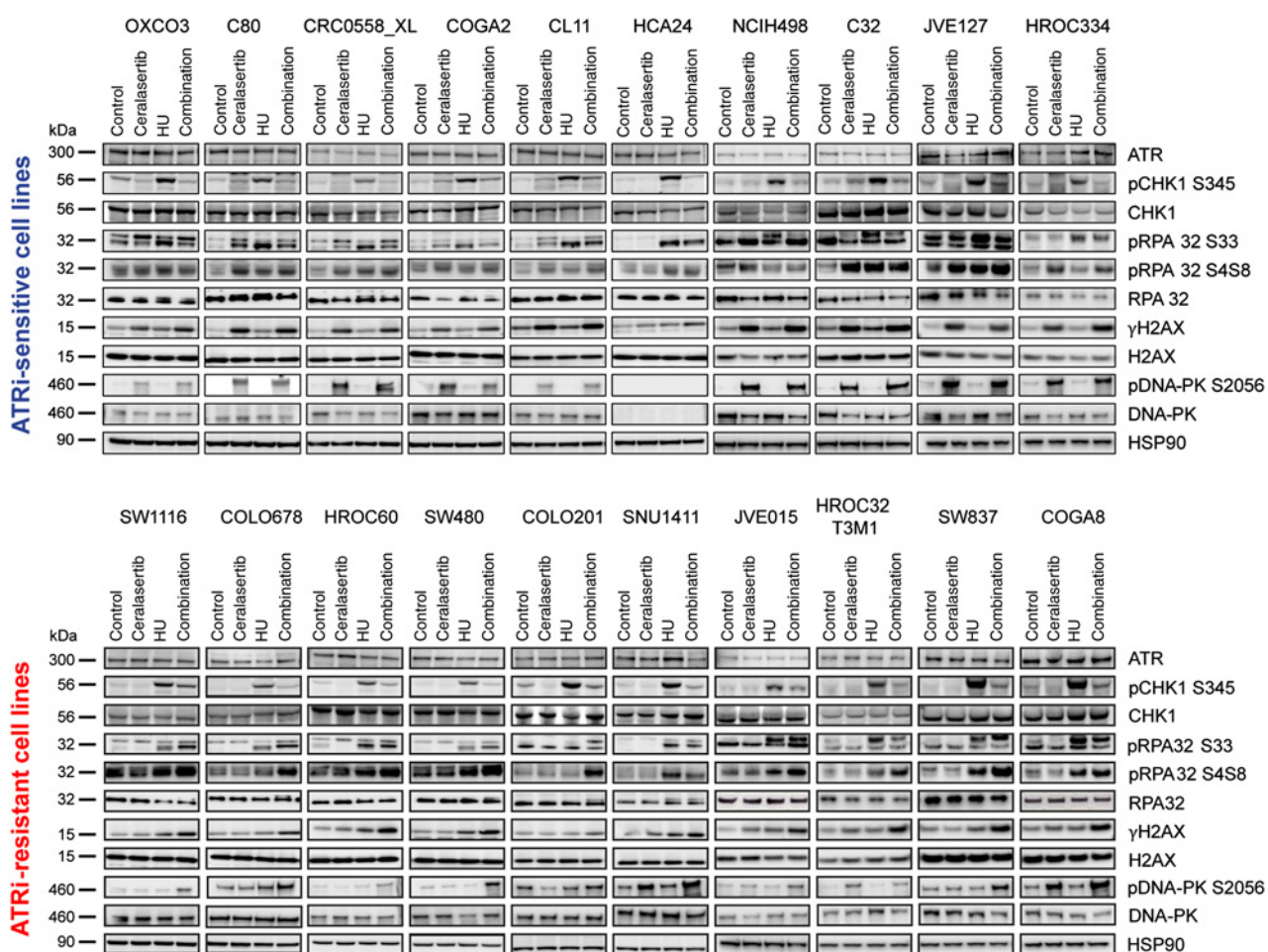


Figure 4.

Q14 Cells sensitive to ATR inhibition exhibit higher levels of endogenous RS activation and DNA-PK activation. The expression and activation/phosphorylation of key players in ATR pathway, RS, NHEJ, and DNA damage was measured by Western blot analysis after 24 hours treatment with 1 μmol/L ATRi ceralasertib, 4 hours HU at a concentration of 2.5 mmol/L, or combination of the two agents (20 hours only ATRi followed by 4 hours ATRi+HU). Cell extracts were immunoblotted with the indicated antibodies and HSP90 was used as a loading control.

627 significantly higher representation of mutational signatures that
 628 are associated with other DNA repair abnormalities in aggregate,
 629 including base excision signatures 18—associated with damage from
 630 8-oxo-dG (8-Oxo-2'-deoxyguanosine), signature 30 due to NTHL1
 631 deficiency, and signature 36 due to MUTYH loss and HR repair
 632 (signatures 3 and 8) deficiencies ($P = 0.0186$). Of note, HRDetect
 633 high scores appeared to identify models with high sensitivity to ATR
 634 blockade, as HROC278MET, KP363T, and HROC334 exhibited the
 635 highest HRDetect scores and were sensitive to this DDRi (Fig. 5E
 636 and F; Supplementary Table S2). Thus, mutational signature analysis

may be a useful tool in revealing defective DDR mechanisms in
 colorectal cancer samples even when a matched normal sample is
 not available.

Testing DDRi in clinically relevant colorectal cancer models

To extend our findings of putative biomarkers of response to ATRi to more clinically relevant models, we tested DDRi in PDOs in which sensitivity to olaparib and oxaliplatin had been determined previously (12). Three of five PDOs (Patient #1, #2, #3) were sensitive to ATR pathway inhibition (Fig. 6A and B; Supplementary Fig. S14). More in

638
 639
 640
 641
 642
 643
 644
 645
 646

Figure 3.

Cells resistant to ATR inhibition exhibit higher levels of endogenous RS and increased RAD51 activity upon exogenous induction of RS. **A**, Immunofluorescence detection of basal pRPA32 foci in ATRi-sensitive (blue histograms) and ATRi-resistant (red histograms) cell models was performed and quantified (at least 400 nuclei were counted for each cell line in two biological replicates). **B**, Statistical significance for basal pRPA32 foci formation between ATRi-sensitive versus ATRi-resistant cell models was calculated using the Mann-Whitney test. Statistical significance: ****, $P < 0.0001$. **C**, Representative images of immunofluorescence staining of pRPA32 foci at basal levels in two ATRi-sensitive and two ATRi-resistant models. DAPI was used to stain nuclei. Magnification: 40×, scale bar: 25 μm. **D**, ATRi-sensitive and ATRi-resistant cell models were treated with 2.5 mmol/L HU for 24 hours. Following treatment, immunofluorescent detection of RAD51 foci formation was performed and compared with untreated cells. **E**, Statistical significance for RAD51 foci formation upon 24 hours HU treatment between ATRi-sensitive versus ATRi-resistant cell models was calculated using the Mann-Whitney test. Statistical significance: ****, $P < 0.0001$. **F**, Representative images of immunofluorescence staining of RAD51 foci after 24 hour-long treatment with 2.5 mmol/L HU in two ATRi-sensitive and two ATRi-resistant models. DAPI was used to stain nuclei. Magnification: 40×, scale bar: 25 μm. For images from the full experiment, please see Supplementary Fig. S5.

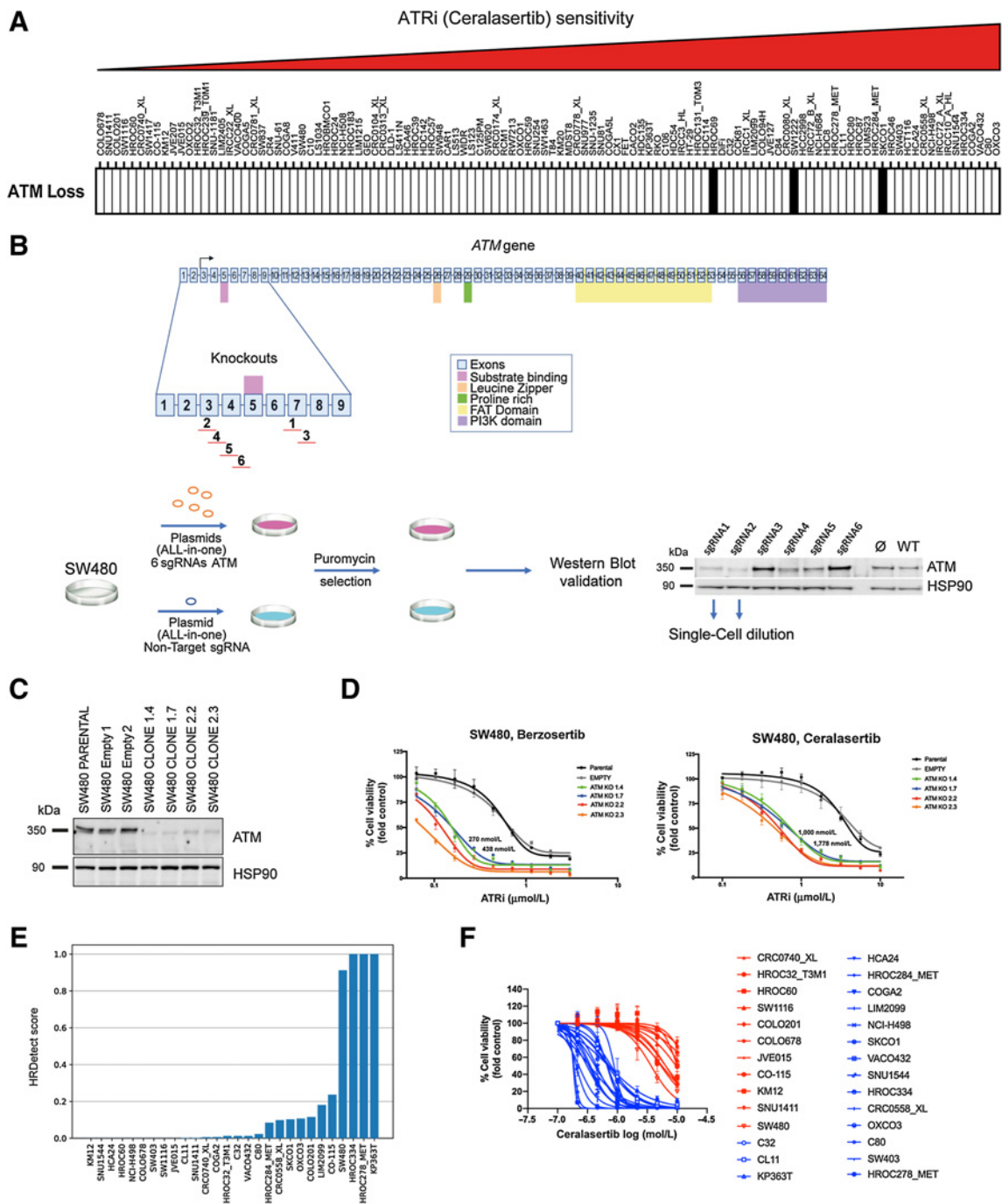


Figure 5.

ATM protein loss and HRDetect analysis identify colorectal cancer sensitive to ATR inhibition. **A**, Identification of three colorectal cancer cell lines (black bar) with complete ATM protein loss (see Supplementary Fig. S12) and response to ATR blockade by ceralasertib. Colorectal cancer cell lines were ranked based on sensitivity to this ATRi calculated on normalized AUC values. **B**, CRISPR/Cas9 KO of ATM gene by six different sgRNAs targeting different exons in ATRi-resistant colorectal cancer cell line SW480. After puromycin selection of single-cell clones and Western blot validation, clones of sgRNA1 and 2 were selected for further single-cell dilution. **C**, Western blot validation of ATM KO of four different single-cell clones. SW480 parental cell line and two empty sgRNAs were used as negative controls. HSP90 was used as a loading control of the immunoblotting. **D**, ATRi testing in ATM KO clones by a 7-day-long cell viability assay. Parental cell line SW480 and isogenic SW480 with empty guide were used as controls. Clinically relevant concentration range of inhibitors (around 300 nmol/L in case of berzosertib and around 1,000 nmol/L for ceralasertib) are highlighted. A representative experiment of three independent biological replicates with technical triplicates is shown. **E**, Bar plot representing the HRDetect score of 28 colorectal cancer cell lines ordered from the lowest to the highest score across the x axis from left to right. **F**, Ceralasertib viability curves in depicted 28 cell lines from **E** after 7-day-long treatment (data coming from **Fig. 2** and Supplementary Fig. S1). Clinically relevant concentration of 1 μmol/L was used as a cutoff to define sensitive models (viability <35%, in blue) compared with the resistant (viability >75%, in red).

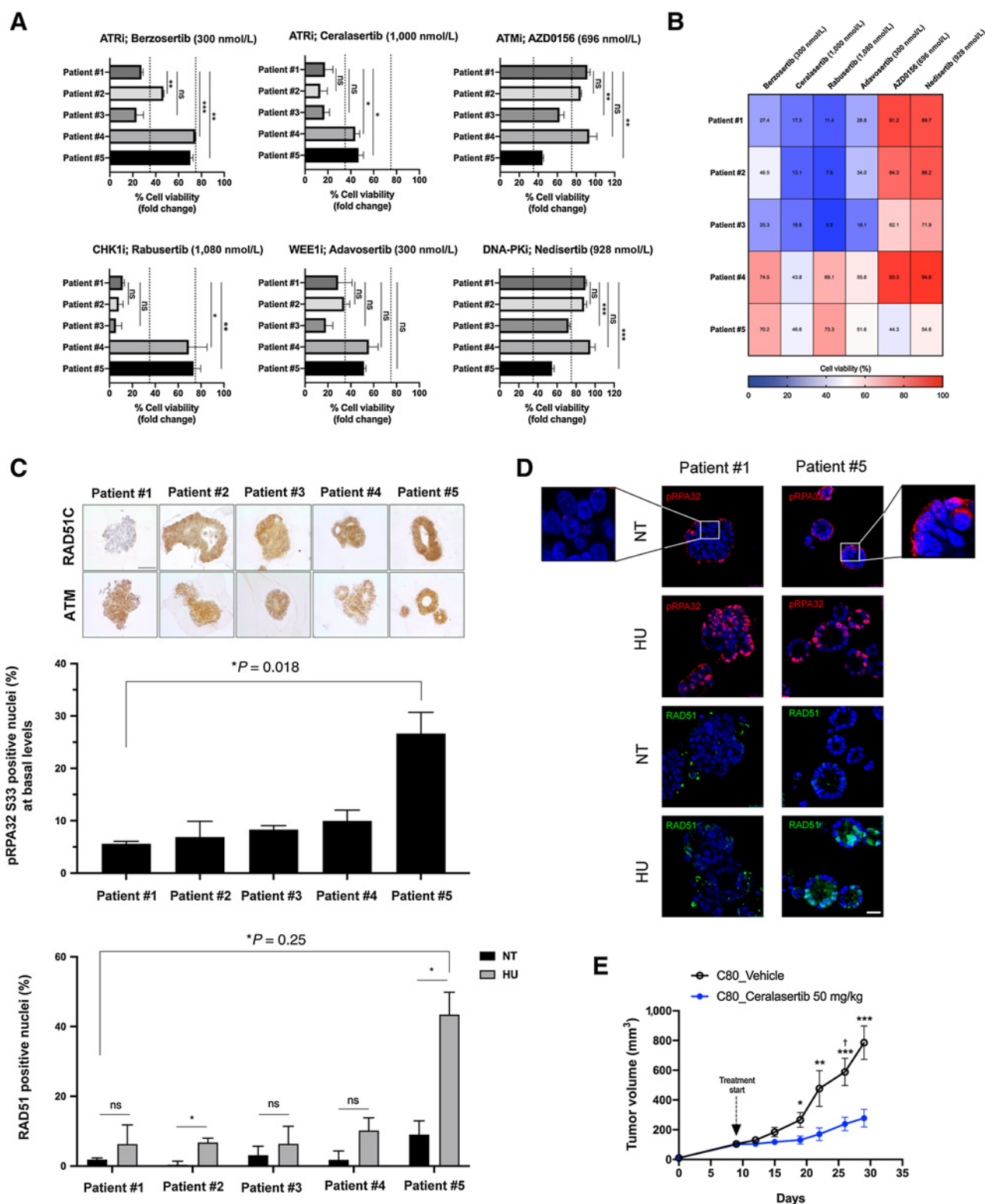


Figure 6. PDOs and PDXs represent clinically relevant models for determination of sensitivity to DDRi *in vitro* and *in vivo*. **A**, Pharmacologic testing of organoids derived from patients with colorectal cancer with six different DDRis in a 7-day-long viability assay. The results at the endpoint were normalized to control wells containing DMSO vehicle and were plotted as histograms (a percent of viability) at clinically relevant concentrations of individual inhibitors. MG-132 was used as a positive control for organoid death (Supplementary Fig. S14). (Continued on the following page.)

649 general, when comparing these results with sensitivity to FOLFIRI/
650 FOLFOX according to the clinical history of the corresponding
651 patients (Supplementary Table S4 in ref. 12), we found out that these
652 same three organoids were those that previously responded to che-
653 motherapy, thus suggesting that potential DDR deficiency might
654 confer cross-sensitivity to both chemotherapeutics and DDRi. To
655 corroborate the insights gathered from cell line analysis, we performed
656 foci analysis upon HU treatment also in PDOs. We observed concor-
657 dant results showing lower basal level of pRPA32 foci and RAD51 foci
658 after 24 hours of HU exposure in the ATRi-sensitive models
659 (Patient#1-2-3), supporting HR deficiency (12) as a biomarker of
660 response to ATR inhibition, although insufficient to make any solid
661 statistical statement due to the limited size of the cohort (Fig. 6C
662 and D). Interestingly, the oxaliplatin- and olaparib-sensitive Patient#1
663 (as characterized in ref. 12), who also responded to previous FOLFIRI
664 treatment, was characterized by loss of RAD51C expression (Fig. 6C),
665 suggesting again the loss of this paralog as a putative biomarker of
666 response to both PARPi and ATRi. Patient#4, who showed a pRPA32
667 and RAD51 profile similar to the ATR-sensitive patients, was resistant
668 to ATRi and PARPi, but sensitive to SN-38 (Supplementary Fig. S15),
669 suggesting that HR-proficient tumors might still be sensitive to
670 topoisomerase I inhibition.

671 Finally, we assessed the sensitivity to the single-agent ceralasertib
672 *in vivo* using a colorectal xenograft model corresponding to one of the
673 cell lines (C80) that we found sensitive to ATR inhibition in our
674 screening (Fig. 2). *In vivo* treatment with ceralasertib led to significant
675 growth control (Fig. 6E) and was well tolerated (Supplementary
676 Fig. S16).

677 Discussion

678 The last decade has seen an unprecedented opportunity for the
679 development of drugs targeting DDR, and numerous clinical trials are
680 currently assessing their efficacy in various types of malignancies,
681 including colorectal cancer (13, 58). Encouraging results are emerging
682 from different tumors, and development of DDRi in colorectal cancer
683 is confined to investigations in a limited number of preclinical models
684 or in few trials (13, 15, 17), where the identification of robust
685 biomarkers of response still remains an urgent clinical need. Here,
686 we present results obtained from, to our knowledge, the first large-scale
687 screening of colorectal cancer preclinical models with seven different
688 DDRi currently being tested in phase I–III clinical trials. In parallel, to
689 identify potentially relevant translational correlations, we have per-
690 formed a screening with the three most used chemotherapeutic agents
691 for colorectal cancer treatment (5-FU, SN-38, and oxaliplatin), thus
692 providing a unique platform of response to agents directly targeting
693 DNA or DDR. We selected 112 colorectal cancer cell lines closely
694 recapitulating the genomic landscape of this tumor type, with a specific
695 enrichment for *RAS/BRAF*-mutant models that remain an unmet need

697 in metastatic colorectal cancer due to their unresponsiveness to
698 targeted therapies such as cetuximab or panitumumab. Pharmacologic
699 analysis unveiled that around 30% of the models are sensitive to at least
700 one DDRi, suggesting that severe impairment to the DDR machinery
701 in colorectal cancer cells renders these tumors vulnerable, in particular
702 with respect to ATR pathway inhibitors (18%–25%). Interestingly, we
703 previously showed in a comparable screening that the number of cells
704 showing sensitivity to PARPi is approximately half of that we observed
705 targeting RS response effectors (12), suggesting a higher incidence of
706 RS defects compared with HR, at least in colorectal cancer, that could
707 be further exploited for therapeutic intervention. The linear correla-
708 tion between sensitivity to SN-38 and ATRi is also of potential clinical
709 relevance. SN-38 is the active metabolite of irinotecan, a standard-of-
710 care drug in metastatic colorectal cancer targeting topoisomerase I
711 (TOP1), which is a crucial component of the DNA replication
712 machinery. This correlation cannot be surprising considering that
713 many of these cell lines are characterized by oncogenic activation that
714 historically has been proven to trigger RS. It derives that inhibition of
715 the RS master regulator ATR has emerged as a top candidate gene for
716 synthetic lethality approaches with TOP1 inhibitors (59) and this
717 supports the design of effective combinatorial strategies involving
718 irinotecan and ATRi (60), whose testing is currently beyond the scope
719 of this article.

720 Given its pivotal role in the RS response, ATR has become an
721 attractive target for the development of small-molecule inhibitors, and
722 many of them are currently being tested in clinical trials as single agent
723 or in combination with other DNA-damaging agents (17, 42). Under-
724 standing the mechanisms and identifying biomarkers that predict
725 response to ATRi would improve patients' stratification and the
726 clinical decision-making process. With this purpose, we have initially
727 focused our investigation on the main players involved in the RS
728 response and found that ATRi-resistant cells exhibit higher basal levels
729 of pRPA32. Previous studies have provided a prognostic significance to
730 RPA1 or RPA2 in different tumor types, including colorectal cancer
731 (61). These and our findings might support the fact that tumors
732 carrying higher levels of RPA could be more tolerant to RS. Given that
733 each cell has a finite pool of RPA for interactions with ssDNA and that
734 ATR recruitment and activation is dependent on this interaction, low
735 levels or exhaustion of RPA might explain the sensitivity of some
736 cancer cells to ATRi (62).

737 We also found that ATRi-resistant cells expressed significantly
738 higher levels of RAD51 foci upon HU treatment, suggesting that
739 these cells might rely on RAD51 and HR-mediated mechanisms to
740 overcome DNA damage and RS. Interestingly, we observed the
741 same trend in a very limited set of PDOs that we screened with
742 DDRi. Overall, these data might pose the preclinical evidence for
743 testing for pRPA32 foci at basal level in patient tumor biopsy
744 samples or patient-derived models (63) to potentially identify those
745 who could likely respond to ATRi (Fig. 7), similarly to other clinical

(Continued.) The screening detected strong pattern of sensitivity to ATRi, CHK1i, and WEE1i in 3 patients (#1–3). Sensitivity cutoff was set to 35% and resistance is above 75% viability (indicated with dashed lines). Unpaired Student *t* test was used for statistical evaluation of the results. ns, nonsignificant. **B**, The heatmap with indicated viability values in percentage at the end of the experiment for indicated drug concentrations. Results (**A** and **B**) are an average of at least two independent biological experiments with technical quadruplicates. Z factor values varied between 0.74 and 0.94. **C**, IHC detection of RAD51C and ATM protein in colorectal cancer PDOs' cytoclots. Patient #1 displays RAD51C negativity compared with other PDOs, while all *ex vivo* tumor models display ATM positivity. The sections were counterstained with hematoxylin. Scale bar: 50 μ m. Quantification of two independent biological experiments performed for detection of pRPA32 S33 foci at basal levels or RAD51 foci after 24-hour-long HU treatment; NT, nontreated. Statistical significance: *, $P < 0.05$; ns, nonsignificant (two-tailed unpaired Student *t* test). **D**, Representative images of immunofluorescence detection of RAD51 and pRPA32 S33 signal in ATRi-resistant (Patient #5) and ATRi-sensitive (Patient #1) organoids treated with 2.5 mmol/L HU for 24 hours. Scale bar: 25 μ m. NT, nontreated; HU, hydroxyurea. **E**, ATRi-sensitive C80 cells were injected into NOD-SCID mice to establish a xenograft growth. After expansion and randomization when the tumor volume in individual mice reached 100/200 mm³, mice started being treated with ceralasertib (50 mg/kg, by oral administration daily) for 21 days. Tumor volumes were measured every 3 days using caliper. \square : one mouse from the control group was sacrificed because of tumor growth reaching the endpoint. Bars, \pm SE. Statistical significance: *, $P < 0.05$; **, $P < 0.01$; ***, $P < 0.001$ (Mann–Whitney nonparametric test).

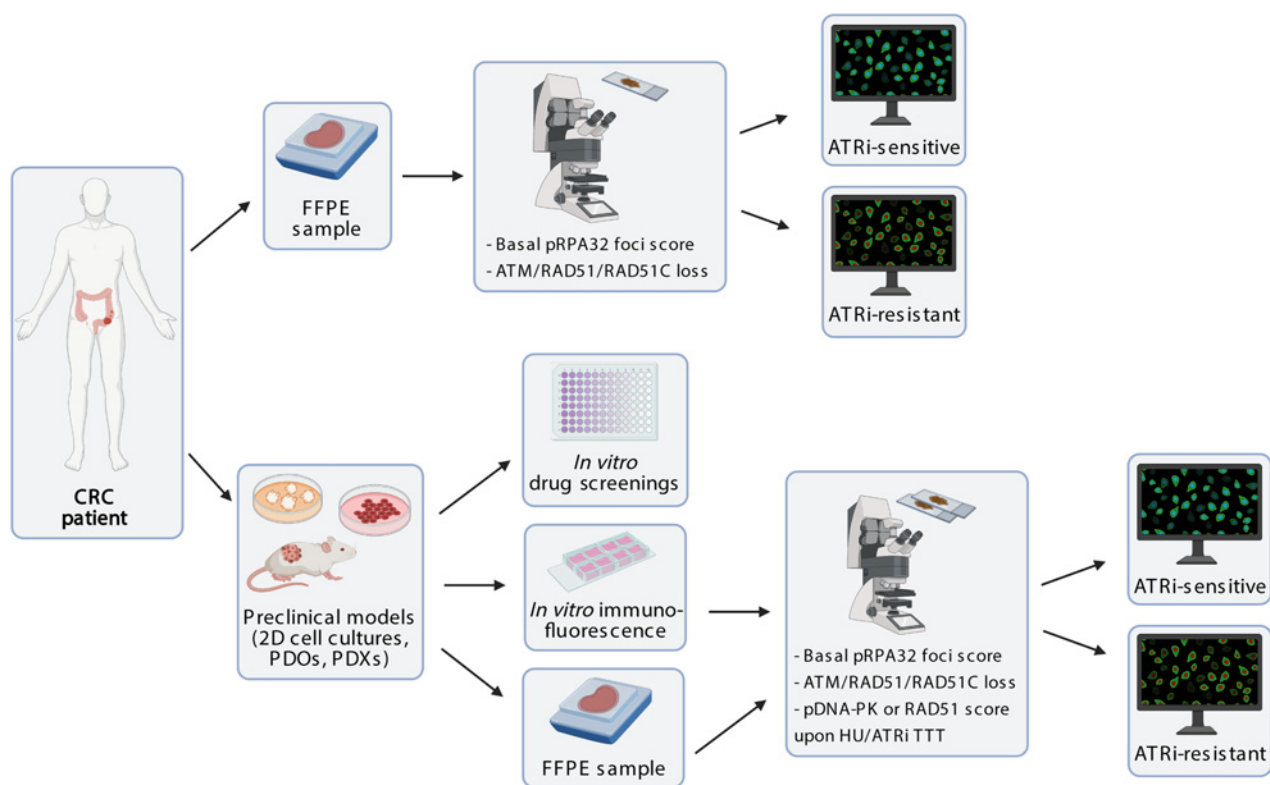


Figure 7.

The proposed preclinical and clinical flow to potentially predict ATRi-sensitive and ATRi-resistant colorectal cancer tumors. After written consent of the patient, tumor sample can be either processed as FFPE sample for direct immunohistologic and immunofluorescence analysis, or preclinical models for *in vitro* and *in vivo* analyses can be established. Samples can be tested for direct *in vitro* drug screenings or for biomarkers analysis through immunofluorescence or IHC assays. To evaluate the relevance of the “composite biomarker” of sensitivity to ATR inhibition, we propose to detect the expression level of proteins ATM, RAD51, and RAD51C together with scoring of phosphor-RPA32 at basal level—prior to treatment. Also, scoring of activated DNA-PK and RAD51 upon treatment with ATRi will be informative. This information may eventually lead to the identification of patients who might benefit from ATR inhibition monotherapy, and directly translate the knowledge from bench to bedside. TTT, treatment. This figure was created with biorender.com. FFPE, formalin-fixed paraffin embedded.

748 analyses where RAD51 foci identified PARPi-vulnerable tumors in
749 breast cancer (64).

750 Considering that genetic data analysis is not sufficient to faithfully
751 predict the real DNA repair capability of a tumor, especially
752 due to the presence of multiple uncharacterized variants of
753 unknown significance, functional testing on a patient-derived platform
754 would be extremely helpful to guide treatment choice, particularly
755 if implemented by the choice of a peculiar clinical setting (13). From
756 a practical point of view, one important limitation of this application
757 could be the difficulty in identifying a clear-cut threshold level to
758 support a yes or no decision for patient selection. An extended analysis
759 in a larger cohort of clinically and molecularly annotated organoids and
760 patients’ tumor samples is warranted to translate these findings to a
761 clinical decision level.

762 Phospho-RPA32 and RAD51 foci levels might be used together with
763 other putative biomarkers that have been previously correlated with
764 sensitivity to ATR inhibition, such as ATM protein loss (52). Accordingly,
765 we propose that analysis of multiple DDR effectors could be combined
766 to generate a “composite” biomarker that more effectively pinpoints
767 patients likely to respond to ATRi (Fig. 7). Here we validated the ATM
768 loss as a biomarker of ATRi sensitivity also in colorectal tissue. Because
769 of the prevalence of this alteration [8%–20% (65, 66)] in the colorectal
770 setting, a significant group of patients

could potentially benefit from ATRi treatment. Because HR and RS
772 are two closely connected pathways, we reasoned that tumors with
773 HR deficiencies might be cross-sensitive to PARPi and ATRi. Accordingly,
774 cells with ATM loss that in our previous screening resulted sensitive to
775 olaparib (12), and here responded to ATRi, suggest that combination
776 of PARPi with RS response inhibitors might be very effective in
777 colorectal cancer, as also observed in other tissues (6). The same was
778 true also for other models that, by means of transcriptomic analysis,
779 we found being with very low or complete loss of expression levels
780 of *RAD51* or *RAD51C*, a *RAD51* paralog with key functions in HR (67).
781 While *RAD51* is an essential gene and many companies are already
782 attempting the development of specific inhibitors, *RAD51C* remains
783 still untargetable and its loss detection might identify those patients
784 with colorectal cancer very likely to respond to ATRi, beyond PARPi.
785

786 On the practical side, assessment of ATM and *RAD51C* might result
787 more easily informative respect to the functional evaluation of pRPA32
788 and *RAD51* due to their clear on/off interpretation.

789 Interestingly, *ATM*, *RAD51*, and *RAD51C* are among the molecular
790 markers that define the *BRCAness* phenotype (also referred to as
791 *HRDness*), and that are evaluated in panel-based companion
792 diagnostic tools used in the clinic to predict HR and to assess patient
793 eligibility for treatment with PARPi (13). More recently, advanced
794

797	signature analysis in breast cancer through the HRDetect score has	(ID. 21091 program) during the conduct of the study; grants from Fondazione AIRC,	859
798	pointed out <i>RAD51C</i> loss as a reliable <i>BRCAness</i> biomarker (68),	Associazione Italiana per la Ricerca sul Cancro, AIRC Investigator Grant 21407	860
799	suggesting that similar molecular approaches could be attempted in	and Italian Ministry of Health - TRANSCAN-2 - THRUSt outside the submitted	861
800	patients with colorectal cancer to further improve patients' selec-	work. A. Bardelli reports grants, personal fees, and non-financial support from	862
801	tion. Here we have presented HRDetect score analysis performed for	Neophore; grants from AstraZeneca, Boehringer; personal fees from Illumina,	863
802	the first time without a germline reference in colorectal cancer models.	Guardant Health; personal fees and non-financial support from Inivata; and non-	864
803	This analysis revealed four cell lines as potential HR defective; while	financial support from Roche/Genentech global colorectal cancer outside the sub-	865
804	three of four resulted sensitive to ATR inhibition, and interestingly	mitted work. S. Arena reports grants from Fondazione AIRC, Associazione Italiana	866
805	they are characterized by the lack of <i>RAD51C</i> expression. On the other	per la Ricerca sul Cancro, AIRC under MFAG 2017-ID 20236 project, grants from	867
806	hand, one cell line (SW480) was resistant to the clinically relevant	FPRC 5xmille 2017 Ministero Salute PTCRC-Intra 2020 (REGENERATION-YIG	868
807	concentration of ceralasertib (1 $\mu\text{mol/L}$), but showed sensitivity to	2020 project), and University of Torino, Department of Oncology, Ricerca Locale	869
808	higher concentrations. Thinking about the limitation to this approach,	2020 and 2021 (premiabilità pubblicazioni) during the conduct of the study; personal	870
809	it should be taken into account that HRDetect is able to identify	fees from MSD Italia outside the submitted work; in addition, S. Arena has a patent	871
810	previous genomic "scars" of HR deficiency that could have evolved	102022000007535 pending. No disclosures were reported by the other authors.	Q19,72
811	during treatment exposure leading to functionally HR-proficient		
812	tumor resistant to the therapy (57).		
813	Extended mutational signature analysis further pointed out higher	Authors' Contributions	873
814	representation of the BER signature in ATRi-sensitive cell lines.	E. Durinikova: Conceptualization, data curation, formal analysis, validation,	874
815	Considering the close interconnection between HR and RS pathways,	investigation, visualization, methodology, writing-review and editing. N.M. Reilly:	875
816	and in particular the role of PARP in cellular processing of DNA	Data curation, validation, investigation, visualization, methodology. K. Buzo: Inves-	876
817	damage through the BER pathway (69), we might exploit this genomic	tigation. E. Mariella: Data curation, formal analysis, investigation, visualization,	877
818	analysis together with composite biomarker testing to significantly	methodology. R. Chilà: Data curation, investigation. A. Lorenzato: Data curation,	878
819	improve and refine patient stratification.	formal analysis, validation, visualization, methodology. J.M.L. Dias: Formal analysis,	879
820	One important limitation of this work is that <i>in vitro</i> experiments	investigation, methodology. G. Grasso: Investigation, visualization. F. Pisati: Data	880
821	have been performed keeping preclinical models (cell lines and	curation, formal analysis, visualization, methodology. S. Lamba: Investigation,	881
822	organoids) in incubators at standard oxygen concentrations (around	methodology. G. Corti: Investigation. A. Degasperì: Formal analysis, investigation,	882
823	20%), which might not completely recapitulate the hypoxic conditions	methodology. C. Cancelliere: Resources. G. Mauri: Investigation. P. Andrei: Data	883
824	of colorectal cancer tissues; high pO_2 could in fact exert DNA damage	curation, visualization. M. Linnebacher: Resources. S. Marsoni: Writing-review and	884
825	that might increase sensitivity to DDRi. However, we were able to show	editing. S. Siena: Resources, funding acquisition. A. Sartore-Bianchi: Resources,	885
826	that even at high pO_2 conditions, subsets of very sensitive as well as	funding acquisition. S. Nik-Zainal: Data curation, formal analysis, supervision,	886
827	very resistant models to DDRi could be identified. In addition, our	funding acquisition, methodology, writing-review and editing. F. Di Nicolantonio:	887
828	successful testing of single ATRi in a xenograft model has also	Funding acquisition, investigation. A. Bardelli: Conceptualization, resources,	888
829	suggested that preselection for RS sensitivity through the "composite"	supervision, funding acquisition, writing-review and editing. S. Arena: Concep-	889
830	biomarker analysis might improve efficacy of the treatment, poten-	tualization, resources, data curation, formal analysis, supervision, funding	890
831	tially even more if in combination or during sequential treatment with	acquisition, investigation, visualization, writing-original draft, project adminis-	891
832	other agents.	tration, writing-review and editing.	Q20,92
833	In conclusion, we provide preclinical evidence showing the efficacy	Acknowledgments	893
834	of novel promising agents targeting DDR and RS in colorectal cancer.	This work was supported, in part, by Fondazione AIRC under 5 per Mille 2018-ID.	894
835	Furthermore, we have identified a "composite" biomarker including	21091 program-P.I. Bardelli Alberto, G.L. Siena Salvatore, G.L. Di Nicolantonio	895
836	different effectors of DNA repair deficiency and RS response (basal	Federica, G.L. Marsoni Silvia; Fondazione Regionale Ricerca Biomedica Regione	896
837	<i>pRPA32</i> , <i>RAD51</i> upon HU, ATM loss, and <i>RAD51C</i> loss), and	Lombardia (Project CP 12/2018 IANG CRC) to S. Siena and A. Sartore-Bianchi; AIRC	897
838	mutational signature analysis as potential predictors of response to	under MFAG 2017-ID 20236 project-P.I. Arena Sabrina; FPRC 5xmille 2017 Min-	898
839	specific DDRi and, more broadly, as biomarkers to define distinct class	istero Salute PTCRC-Intra 2020 (REGENERATION-YIG 2020 project) to S. Arena;	899
840	of patients with unique vulnerabilities in the DDR pathways. Further	Ricerca Locale 2020 and 2021 (premiabilità pubblicazioni)-University of Torino, Dept	900
841	investigation with combinatorial strategies is warranted to maximize	of Oncology to S. Arena; AIRC IG 2018-ID. 21923 to A. Bardelli.; AIRC IG (no. 20685)	901
842	DDR-targeting effects in colorectal cancer. These preclinical results	to S. Siena; Terapia Molecolare Tumori by Fondazione Oncologia Niguarda Onlus to	902
843	could inform future testing of DDRi in selected cohorts of patients with	A. Sartore-Bianchi and S. Siena; International Accelerator Award, ACRCELERATE,	903
844	colorectal cancer.	jointly funded by Cancer Research UK (A26825 and A28223), FC AECC	904
845	Authors' Disclosures	(GEACC18004TAB) and AIRC (22795) to A. Bardelli; Ministero Salute, RC 2020	905
846	N.M. Reilly is currently an employee of Cytir Therapeutics and the entirety of his	to A. Bardelli; the project leading to this application has received funding from the	906
847	contribution to the submitted work was performed prior to his current employment.	European Research Council (ERC) under the European Union's Horizon 2020	907
848	A. Degasperì reports other support from CRUK outside the submitted work; in	research and innovation programme (grant agreement no 101020342) to A. Bardelli;	908
849	addition, A. Degasperì has a patent for HRDetect pending to CRUK. S. Siena reports	E. Mariella was supported by the FIRC-AIRC "Michele e Carlo Arduzzone" fellowship	909
850	other support from Agenus, AstraZeneca, BMS, CheckmAb, Daiichi-Sankyo, Guard-	for Italy. S. Nik-Zainal, A. Degasperì, and J.M.L. Dias are funded by a CRUK	910
851	ant Health, Menarini, Merck, Novartis, Roche-Genentech, and Seagen outside the	Advanced Clinician Scientist Award C60100/A23916, CRUK Early Detection Project	911
852	submitted work. A. Sartore-Bianchi reports personal fees from Amgen, Bayer,	award C60100/A27815 and supported by National Institute of Health Research	912
853	Novartis, and Servier outside the submitted work. S. Nik-Zainal reports grants from	(NIHR) Cambridge Biomedical Research Centre grant BRC-125-20014.	913
854	CRUK, Dr Josef Steiner Foundation, and NIHR during the conduct of the study; other	The authors wish to thank V. Costanzo and F. D'Adda di Fagagna (IFOM - the	914
855	support from SABCS outside the submitted work; in addition, S. Nik-Zainal has a	FIRC Institute of Molecular Oncology - Milan, Italy) for their critical reading of the	915
856	patent for HRDetect pending. F. Di Nicolantonio reports grants from Fondazione	manuscript and insightful suggestions. The authors also thank members of the	916
857	AIRC, Associazione Italiana per la Ricerca sul Cancro, AIRC under 5 per Mille 2018	Molecular Oncology Laboratory at Candiolo Cancer Institute for scientific support	917
		and critical reading of the article.	918
		The costs of publication of this article were defrayed in part by the payment of page	919
		charges. This article must therefore be hereby marked <i>advertisement</i> in accordance	920
		with 18 U.S.C. Section 1734 solely to indicate this fact.	921
		Received March 18, 2022; revised May 5, 2022; accepted July 1, 2022; published first	922
		xx xx, xxxx.	923

92(Q21

References

1. Hanahan D, Weinberg RA. Hallmarks of cancer: the next generation. *Cell* 2011; 144:646–74. 927
2. Pearl LH, Schierz AC, Ward SE, Al-Lazikani B, Pearl FMG. Therapeutic opportunities within the DNA damage response. *Nat Rev Cancer* 2015;15: 166–80. 929
3. Mateo J, Lord CJ, Serra V, Tutt A, Balmaña J, Castroviejo-Bermejo M, et al. A decade of clinical development of PARP inhibitors in perspective. *Ann Oncol* 2019;30:1437–47. 930
4. Yap TA, Plummer R, Azad NS, Helleday T. The DNA damaging revolution: PARP inhibitors and beyond. *Am Soc Clin Oncol Educ Book* 2019;39:185–95. 931
5. Berti M, Vindigni A. Replication stress: getting back on track. *Nat Struct Mol Biol* 2016;23:103–9. 932
6. Ngoi NYL, Pham MM, Tan DSP, Yap TA. Targeting the replication stress response through synthetic lethal strategies in cancer medicine. *Trends Cancer* 2021;7:930–57. 933
7. Pilić PG, Tang C, Mills GB, Yap TA. State-of-the-art strategies for targeting the DNA damage response in cancer. *Nat Rev Clin Oncol* 2019;16:81–104. 934
8. Rospo G, Lorenzato A, Amirouchene-Angelozzi N, Magri A, Cancelliere C, Corti G, et al. Evolving neoantigen profiles in colorectal cancers with DNA repair defects. *Genome Med* 2019;11:42. 935
9. André T, Shiu KK, Kim TW, Jensen BV, Jensen LH, Punt C, et al. Pembrolizumab in microsatellite-instability-high advanced colorectal cancer. *N Engl J Med* 2020; 383:2207–18. 936
10. Di Nicolantonio F, Vitiello PP, Marsoni S, Siena S, Tabernero J, Trusolino L, et al. Precision oncology in metastatic colorectal cancer - from biology to medicine. *Nat Rev Clin Oncol* 2021;18:506–25. 937
11. Argiles G, Arnold D, Prager G, Sobrero AF, Van Cutsem E. Maximising clinical benefit with adequate patient management beyond the second line in mCRC. *ESMO Open* 2019;4:e000495. 938
12. Arena S, Corti G, Durinikova E, Montone M, Reilly NM, Russo M, et al. A subset of colorectal cancers with cross-sensitivity to olaparib and oxaliplatin. *Clin Cancer Res* 2020;26:1372–84. 939
13. Mauri G, Arena S, Siena S, Bardelli A, Sartore-Bianchi A. The DNA damage response pathway as a land of therapeutic opportunities for colorectal cancer. *Ann Oncol* 2020;31:1135–47. 940
14. Moretto R, Elliott A, Zhang J, Arai H, Germani MM, Conca V, et al. Homologous recombination deficiency alterations in colorectal cancer: clinical, molecular, and prognostic implications. *J Natl Cancer Inst* 2022;114:271–9. 941
15. Manic G, Signore M, Sistigu A, Russo G, Corradi F, Siteni S, et al. CHK1-targeted therapy to deplete DNA replication-stressed, p53-deficient, hyperdiploid colorectal cancer stem cells. *Gut* 2018;67:903–17. 942
16. Seligmann JF, Fisher DJ, Brown LC, Adams RA, Graham J, Quirke P, et al. Inhibition of WEE1 is effective in TP53- and RAS-mutant metastatic colorectal cancer: a randomized trial (FOCUS4-C) comparing adavosertib (AZD1775) with active monitoring. *J Clin Oncol* 2021;39:3705–15. 943
17. Yap TA, Krebs MG, Postel-Vinay S, El-Khouiery A, Soria JC, Lopez J, et al. Ceralasertib (AZD6738), an oral ATR kinase inhibitor, in combination with carboplatin in patients with advanced solid tumors: a phase I study. *Clin Cancer Res* 2021;27:5213–24. 944
18. Barnieh FM, Loadman PM, Falconer RA. Progress towards a clinically-successful ATR inhibitor for cancer therapy. *Curr Res Pharmacol Drug Discov* 2021;2: 100017. 945
19. Medico E, Russo M, Picco G, Cancelliere C, Valtorta E, Corti G, et al. The molecular landscape of colorectal cancer cell lines unveils clinically actionable kinase targets. *Nat Commun* 2015;6:7002. 946
20. Lazzari L, Corti G, Picco G, Isella C, Montone M, Arcella P, et al. Patient-derived xenografts and matched cell lines identify pharmacogenomic vulnerabilities in colorectal cancer. *Clin Cancer Res* 2019;25:6243–59. 947
21. Corti G, Bartolini A, Crisafulli G, Novara L, Rospo G, Montone M, et al. A genomic analysis workflow for colorectal cancer precision oncology. *Clin Colorectal Cancer* 2019;18:91–101. 948
22. Soneson C, Love MI, Robinson MD. Differential analyses for RNA-seq: transcript-level estimates improve gene-level inferences. *F1000Res* 2015;4:1521. 949
23. Love MI, Huber W, Anders S. Moderated estimation of fold change and dispersion for RNA-seq data with DESeq2. *Genome Biol* 2014;15:550. 950
24. Gu Z, Gu L, Eils R, Schlesner M, Brors B. circlize implements and enhances circular visualization in R. *Bioinformatics* 2014;30:2811–2. 951
25. Gu Z, Eils R, Schlesner M. Complex heatmaps reveal patterns and correlations in multidimensional genomic data. *Bioinformatics* 2016;32:2847–9. 952
26. Li H. Aligning sequence reads, clone sequences and assembly contigs with BWA-MEM; 2013. Available from: <http://arxiv.org/abs/1303.3997>. 997
27. Kim S, Scheffler K, Halpern AL, Bekritsky MA, Noh E, Källberg M, et al. Strelka2: Fast and accurate variant calling for clinical sequencing applications. *Nat Methods* 2018;15:591–4. 998
28. Chen X, Schulz-Trieglaff O, Shaw R, Barnes B, Schlesinger F, Källberg M, et al. Manta: rapid detection of structural variants and indels for germline and cancer sequencing applications. *Bioinformatics* 2016;32:1220–2. 999
29. Sherry ST, Ward MH, Kholodov M, Baker J, Phan L, Smigielski EM, et al. dbSNP: the NCBI database of genetic variation. *Nucleic Acids Res* 2001;29:308–11. 1000
30. Lappalainen I, Lopez J, Skipper L, Hefferon T, Spalding JD, Garner J, et al. DbVar and DGVA: public archives for genomic structural variation. *Nucleic Acids Res* 2013;41:D936–41. 1001
31. Hiltmann S, Jenster G, Trapman J, van der Spek P, Stubbs A. Discriminating somatic and germline mutations in tumor DNA samples without matching normals. *Genome Res* 2015;25:1382–90. 1002
32. Priestley P, Baber J, Lolkema MP, Steeghs N, de Bruijn E, Shale C, et al. Pan-cancer whole-genome analyses of metastatic solid tumours. *Nature* 2019;575: 210–6. 1003
33. Van Loo P, Nordgard SH, Lingjærde OC, Russnes HG, Rye IH, Sun W, et al. Allele-specific copy number analysis of tumors. *Proc Natl Acad Sci U S A* 2010; 107:16910–5. 1004
34. Clarke L, Fairley S, Zheng-Bradley X, Streeter I, Perry E, Lowy E, et al. The international Genome sample resource (IGSR): a worldwide collection of genome variation incorporating the 1000 Genomes Project data. *Nucleic Acids Res* 2017;45:D854–D9. 1005
35. Degasperis A, Amarante TD, Czarnecki J, Shooter S, Zou X, Glodzik D, et al. A practical framework and online tool for mutational signature analyses show inter-tissue variation and driver dependencies. *Nat Cancer* 2020;1:249–63. 1006
36. Tate JG, Bamford S, Jubb HC, Sondka Z, Beare DM, Bindal N, et al. COSMIC: the catalogue of somatic mutations in cancer. *Nucleic Acids Res* 2019;47:D941–D7. 1007
37. Davies H, Glodzik D, Morganello S, Yates LR, Staaf J, Zou X, et al. HRDetect is a predictor of BRCA1 and BRCA2 deficiency based on mutational signatures. *Nat Med* 2017;23:517–25. 1008
38. Sanjana NE, Shalem O, Zhang F. Improved vectors and genome-wide libraries for CRISPR screening. *Nat Methods* 2014;11:783–4. 1009
39. Dienstmann R, Vermeulen L, Guinney J, Kopetz S, Tejpar S, Tabernero J. Consensus molecular subtypes and the evolution of precision medicine in colorectal cancer. *Nat Rev Cancer* 2017;17:79–92. 1010
40. Isella C, Brundu F, Bellomo SE, Galimi F, Zanella E, Porporato R, et al. Selective analysis of cancer-cell intrinsic transcriptional traits defines novel clinically relevant subtypes of colorectal cancer. *Nat Commun* 2017;8: 15107. 1011
41. Mullins CS, Micheel B, Matschos S, Leuchter M, Burtin F, Krohn M, et al. Integrated biobanking and tumor model establishment of human colorectal carcinoma provides excellent tools for preclinical research. *Cancers* 2019;11: 1520. 1012
42. Yap TA, O’Carrigan B, Penney MS, Lim JS, Brown JS, de Miguel Luken MJ, et al. Phase I trial of first-in-class ATR inhibitor M6620 (VX-970) as monotherapy or in combination with carboplatin in patients with advanced solid tumors. *J Clin Oncol* 2020;38:3195–204. 1013
43. van Bussel MTJ, Awada A, de Jonge MJA, Mau-Sørensen M, Nielsen D, Schöffski P, et al. A first-in-man phase 1 study of the DNA-dependent protein kinase inhibitor peposertib (formerly M3814) in patients with advanced solid tumours. *Br J Cancer* 2021;124:728–35. 1014
44. Riches LC, Trinidad AG, Hughes G, Jones GN, Hughes AM, Thomason AG, et al. Pharmacology of the ATM inhibitor AZD0156: potentiation of irradiation and olaparib responses preclinically. *Mol Cancer Ther* 2020;19: 13–25. 1015
45. Bonner WM, Redon CE, Dickey JS, Nakamura AJ, Sedelnikova OA, Solier S, et al. γ H2AX and cancer. *Nat Rev Cancer* 2008;8:957–67. 1016
46. Yates LA, Aramayo RJ, Pokhrel N, Caldwell CC, Kaplan JA, Perera RL, et al. A structural and dynamic model for the assembly of replication protein A on single-stranded DNA. *Nat Commun* 2018;9:5447. 1017
47. Zhang Y, Hunter T. Roles of Chk1 in cell biology and cancer therapy. *Int J Cancer* 2014;134:1013–23. 1018
48. Anantha RW, Sokolova E, Borowiec JA. RPA phosphorylation facilitates mitotic exit in response to mitotic DNA damage. *Proc Natl Acad Sci U S A* 2008;105: 12903–8. 1019

1068	49. Ashley AK, Shrivastav M, Nie J, Amerin C, Troksa K, Glanzer JG, et al. DNA-PK phosphorylation of RPA32 Ser4/Ser8 regulates replication stress checkpoint activation, fork restart, homologous recombination and mitotic catastrophe. <i>DNA Repair</i> 2014;21:131–9.	1100
1069		1101
1070		1102
1071		1103
1072	50. Primo LMF, Teixeira LK. DNA replication stress: oncogenes in the spotlight. <i>Genet Mol Biol</i> 2019;43:e20190138.	1104
1073		1105
1074	51. Lakin ND, Jackson SP. Regulation of p53 in response to DNA damage. <i>Oncogene</i> 1999;18:7644–55.	1106
1075		1107
1076	52. Rafiei S, Fitzpatrick K, Liu D, Cai M-Y, Elmarakeby HA, Park J, et al. ATM loss confers greater sensitivity to ATR inhibition than PARP inhibition in prostate cancer. <i>Cancer Res</i> 2020;80:2094–100.	1108
1077		1109
1078		1110
1079	53. Dunlop CR, Wallez Y, Johnson TI, Bernaldo de Quirós Fernández S, Durant ST, Cadogan EB, et al. Complete loss of ATM function augments replication catastrophe induced by ATR inhibition and gemcitabine in pancreatic cancer models. <i>Br J Cancer</i> 2020;123:1424–36.	1111
1080		1112
1081	54. Khanna KK, Lavin MF, Jackson SP, Mulhern TD. ATM, a central controller of cellular responses to DNA damage. <i>Cell Death Differ</i> 2001;8:1052–65.	1113
1082		1114
1083	55. Min A, Im SA, Yoon YK, Song SH, Nam HJ, Hur HS, et al. RAD51C-deficient cancer cells are highly sensitive to the PARP inhibitor olaparib. <i>Mol Cancer Ther</i> 2013;12:865–77.	1115
1084		1116
1085	56. Alexandrov LB, Kim J, Haradhvala NJ, Huang MN, Tian Ng AW, Wu Y, et al. The repertoire of mutational signatures in human cancer. <i>Nature</i> 2020;578:94–101.	1117
1086		1118
1087	57. Koh G, Degasperi A, Zou X, Momen S, Nik-Zainal S. Mutational signatures: emerging concepts, caveats and clinical applications. <i>Nat Rev Cancer</i> 2021;21:619–37.	1119
1088		1120
1089	58. Brandsma I, Fleuren EDG, Williamson CT, Lord CJ. Directing the use of DDR kinase inhibitors in cancer treatment. <i>Expert Opin Investig Drugs</i> 2017;26:1341–55.	1121
1090		1122
1091	59. Jossé R, Martin SE, Guha R, Ormanoglu P, Pfister TD, Reaper PM, et al. ATR inhibitors VE-821 and VX-970 sensitize cancer cells to topoisomerase I inhibitors by disabling DNA replication initiation and fork elongation responses. <i>Cancer Res</i> 2014;74:6968–79.	1123
1092		1124
1093	60. Thomas A, Pommier Y. Targeting topoisomerase I in the era of precision medicine. <i>Clin Cancer Res</i> 2019;25:6581–9.	1125
1094		1126
1095	61. Dueva R, Iliakis G. Replication protein A: a multifunctional protein with roles in DNA replication, repair and beyond. <i>NAR Cancer</i> 2020;2:zcaa022.	1127
1096		1128
1097	62. Toledo Luis I, Altmeyer M, Rask M-B, Lukas C, Larsen Dorthe H, Povlsen Lou K, et al. ATR prohibits replication catastrophe by preventing global exhaustion of RPA. <i>Cell</i> 2013;155:1088–103.	1129
1098		1130
	63. Durinikova E, Buzo K, Arena S. Preclinical models as patients' avatars for precision medicine in colorectal cancer: past and future challenges. <i>J Exp Clin Cancer Res</i> 2021;40:185.	
	64. Castroviejo-Bermejo M, Cruz C, Llop-Guevara A, Gutiérrez-Enríquez S, Ducey M, Ibrahim YH, et al. A RAD51 assay feasible in routine tumor samples calls PARP inhibitor response beyond BRCA mutation. <i>EMBO Mol Med</i> 2018;10:e9172.	
	65. Sundar R, Miranda S, Rodrigues DN, Chenard-Poirier M, Dolling D, Clarke M, et al. Ataxia telangiectasia mutated protein loss and benefit from oxaliplatin-based chemotherapy in colorectal cancer. <i>Clin Colorectal Cancer</i> 2018;17:280–4.	
	66. Grabsch H, Dattani M, Barker L, Maughan N, Maude K, Hansen O, et al. Expression of DNA double-strand break repair proteins ATM and BRCA1 predicts survival in colorectal cancer. <i>Clin Cancer Res</i> 2006;12:1494–500.	
	67. Sullivan MR, Bernstein KA. RAD-ical new insights into RAD51 regulation. <i>Genes</i> 2018;9:629.	
	68. Staaf J, Glodzik D, Bosch A, Vallon-Christersson J, Reuterswärd C, Hakkinen J, et al. Whole-genome sequencing of triple-negative breast cancers in a population-based clinical study. <i>Nat Med</i> 2019;25:1526–33.	
	69. Horton JK, Stefanick DF, Prasad R, Gassman NR, Kedar PS, Wilson SH. Base excision repair defects invoke hypersensitivity to PARP inhibition. <i>Mol Cancer Res</i> 2014;12:1128–39.	

AUTHOR QUERIES

AUTHOR PLEASE ANSWER ALL QUERIES

- Q1: Page: 1: Author: Per journal style, genes, alleles, loci, and oncogenes are italicized; proteins are roman. Please check throughout to see that the words are styled correctly. AACR journals have developed explicit instructions about reporting results from experiments involving the use of animal models as well as the use of approved gene and protein nomenclature at their first mention in the manuscript. Please review the instructions at <http://aacrjournals.org/content/authors/editorial-policies#genomen> to ensure that your article is in compliance. If your article is not in compliance, please make the appropriate changes in your proof.
- Q2: Page: 1: Author: Please verify the drug names and their dosages used in the article.
- Q3: Page: 1: Author: Please verify the affiliations and their corresponding author links.
- Q4: Page: 1: Author: Please verify the corresponding author details.
- Q5: Page: 1: Author: Please note that abbreviation “MSI” is defined as “microsatellite unstable” here and as “microsatellite instable” later in the text. Please retain single spelled out form.
- Q6: Page: 2: Author: Please define “CHKi,” “ATMi,” “Wee1i,” DNA-PKi.”
- Q7: Page: 3: Author: Should “bwa-mem” be changed to “BWA-MEM” here? Please suggest.
- Q8: Page: 4: Author: Should “xenoorganoids” be changed to “xeno-organoids” here? Please suggest.
- Q9: Page: 4: Author: Should “BME/growth media” be changed to “BME and/or growth media” here? Please suggest.
- Q10: Page: 4: Author: Units of measurement have been changed here and elsewhere in the text from “M” to “mol/L,” and related units, such as “mmol/L” and “ $\mu\text{mol/L}$,” in figures, legends, and tables in accordance with journal style, derived from the Council of Science Editors Manual for Authors, Editors, and Publishers and the Système international d'unités. Please note if these changes are not acceptable or appropriate in this instance.
- Q11: Page: 5: Author: Should “ 5×10^6 ” be changed to “ 5×10^6 ” here? Please suggest.
- Q12: Page: 5: Author: Should “100/200 mm³” be changed to “100–200 mm³” throughout in the text? Please suggest.
- Q13: Page: 6: Author: Please confirm quality/labeling of all images included within this article. Thank you.
- Q14: Page: 9: Author: Should “activation/phosphorylation” be changed to “activation and/or phosphorylation” here? Please suggest.
- Q15: Page: 6: Author: Should “DDR/cell-cycle genes” be changed to “DDR and/or cell-cycle genes” here? Please suggest.
- Q16: Page: 7: Author: Should “analysis” be changed to “analyses” here? Please suggest.

- Q17: Page: 12: Author: Please verify “Patient#1-2-3” for correctness here.
- Q18: Page: 13: Author: Should “on/off” be changed to “on and/or off” here? Please suggest.
- Q19: Page: 14: Author: The Authors' Disclosures statement that appears in the proof incorporates the information from forms completed and signed off on by each individual author. No factual changes can be made to disclosure information at the proof stage. However, typographical errors or misspelling of author names should be noted on the proof and will be corrected before publication. Please note if any such errors need to be corrected. Is the disclosure statement correct?
- Q20: Page: 14: Author: The contribution(s) of each author are listed in the proof under the heading "Authors' Contributions." These contributions are derived from forms completed and signed off on by each individual author. If you make changes to these contributions, you must inform the affected author(s).
- Q21: Page: 15: Author: Note that Refs. 52 and 65 were identical; therefore, the latter has been deleted from the list and subsequent references have been renumbered in both the list and the text. Please verify.

AU: Below is a summary of the name segmentation for the authors according to our records. The First Name and the Surname data will be provided to PubMed when the article is indexed for searching. Please check each name carefully and verify that the First Name and Surname are correct. If a name is not segmented correctly, please write the correct First Name and Surname on this page and return it with your proofs. If no changes are made to this list, we will assume that the names are segmented correctly, and the names will be indexed as is by PubMed and other indexing services.

First Name	Surname		
Erika	Durnikova	Federica	Pisati
Nicole M.	Reilly	Simona	Lamba
Kristi	Buzo	Giorgio	Corti
Elisa	Mariella	Andrea	Degasperi
Rosaria	Chilà	Carlotta	Cancelliere
Annalisa	Lorenzato	Gianluca	Mauri
João M. L.	Dias	Pietro	Andrei
Gaia	Grasso	Michael	Linnebacher

Silvia	Marsoni
Salvatore	Siena
Andrea	Sartore-Bianchi
Serena	Nik-Zainal
Federica Di	Nicolantonio
Alberto	Bardelli
Sabrina	Arena